

UCSF

UC San Francisco Electronic Theses and Dissertations

Title

Active site and ion activation studies on brain and eel acetylcholinesterase

Permalink

<https://escholarship.org/uc/item/14m9160r>

Author

Gordon, Michael Andrew

Publication Date

1976

Peer reviewed|Thesis/dissertation

Active Site and Ion Activation Studies on
Brain and Eel Acetylcholinesterase

by

Michael Andrew Gordon

DISSERTATION

Submitted in partial satisfaction of the requirements for the degree of

DOCTOR OF PHILOSOPHY

in

PHARMACOLOGY

in the

GRADUATE DIVISION

(San Francisco)

of the

UNIVERSITY OF CALIFORNIA



Dedication I

To my mother, Mrs. Louis Gordon

and

to the memory of my father Louis Gordon

TABLE OF CONTENTS

	<u>Page</u>
Acknowledgements	i
List of Tables	ii
List of Figures	iv
Abstract	v
 INTRODUCTION	 1
History	1
Synaptic function	2
Possible enzyme regulatory sites	4
Thermodynamic and kinetic approaches	6
Active site determinations on forms of mammalian brain and eel acetylcholinesterase	8
Questions considered in this study	10
 METHODS	
Materials	11
Active site determinations	11
Preparation of bovine brain and eel acetylcholinesterase forms	11
Purification of ³ H-di-isopropylfluorophosphate	13
Gradient gel electrophoresis of acetylcholinesterase forms	16
Phosphorylation of acetylcholinesterase forms by ³ H- di-isopropylfluorophosphate	21
Active site number for acetylcholinesterase forms	25
Ion activation of acetylcholinesterase	29
Kinetic measurements	29
Determination of acetylation rate constants (k_{+2}), de- acetylation rate constants (k_{+3}), and thermodynamic activation parameters	33
 RESULTS	
Kinetic analysis of calcium activation of brain acetyl- cholinesterase forms	39
Effect of pH on kinetic constants	39
Calcium effects on thermodynamic activation parameters	46
Calcium effects on K_m	46

TABLE OF CONTENTS (continued)

Eel acetylcholinesterase	58
Effect of pH on kinetic constants	58
Calcium effects on thermodynamic activation parameters	61
Calcium effects on K_m	64
Effects of other ions on rate acceleration	64
Gradient gel electrophoresis of brain acetylcholinesterase	69
Time course experiments with forms B and C of brain acetylcholinesterase	69
DISCUSSION	
Thermodynamic and kinetic analysis of Ca^{2+} activation of brain and eel acetylcholinesterase	75
pH dependence of Ca^{2+} influences on acetylcholine hydrolysis by brain and eel acetylcholinesterase	75
Thermodynamic activation parameters and K_m	84
Active site numbers and molecular forms of brain acetylcholinesterase	93
Brain acetylcholinesterase multiple forms and Ca^{2+} acceleration	96
BIBLIOGRAPHY	97
APPENDICES	104

Acknowledgements

I would like to thank the following people for their key help in various aspects of my graduate work at the University of California, San Francisco: Dr. A. J. Trevor, my research supervisor, Dr. S. L. Chan, Dr Eugene Gardner, Dr Wayne Settle, Dr. E.L. Way, Dr. George Ellman, Mr. Chuck Lee, Mr. Leo Davidson, Dr. B. Katzung, and Dr. R. Nicoll. Also, I would like to express appreciation to my fellow students, as well as post-docs and others who made my experience in the Pharmacology Department more enjoyable.

A partial list:

Keith Parker

Don Thorne

Martha

David

LIST OF TABLES

<u>Table</u>		<u>Page</u>
I	Effects of pyridine-2-aldoxime on ^3H -di-isopropylfluorophosphate labelling of eel acetylcholinesterase	22
II	Active site numbers of acetylcholinesterase from eel electric tissue	26
III	Active site numbers of brain acetylcholinesterase forms	28
IV	240000 molecular weight brain acetylcholinesterase form: pH dependence of the overall rate constant (k), acetylation rate constant (k_{+2}), and de-acetylation rate constant (k_{+3})	40
V	240000 molecular weight brain AChE form: pH dependence of the ratios of reaction rate constants in the presence absence of Ca^{2+}	41
VI	60000 molecular weight brain acetylcholinesterase form: pH dependence of the overall rate constant (k), acetylation rate constant (k_{+2}) and de-acetylation rate constant (k_{+3})	43
VII	60000 molecular weight brain AChE form: pH dependence of the ratios of rate constants in the presence and absence of Ca^{2+}	44
VIII	60000 molecular weight brain AChE form: Effect of temperature and Ca^{2+} on the two reaction apparent pK's	48
IX	240000 molecular weight brain acetylcholinesterase form: Thermodynamic activation parameters for acetylation in the presence and absence of Ca^{2+}	49
X	240000 molecular weight brain acetylcholinesterase form: Thermodynamic activation parameters for de-acetylation in the presence and absence of Ca^{2+}	50
XI	60000 molecular weight brain acetylcholinesterase form: Thermodynamic activation parameters for acetylation in the presence and absence of Ca^{2+}	51
XII	60000 molecular weight brain acetylcholinesterase form: Thermodynamic activation parameters for de-acetylation in the presence and absence of Ca^{2+}	52
XIII	240000 molecular weight brain acetylcholinesterase form: Influence of pH and Ca^{2+} on the apparent K_m	53

LIST OF TABLES (continued)

<u>Table</u>		<u>Page</u>
XIV	240000 molecular weight brain AChE form: Influence of pH and Ca^{2+} on the derived $\underline{K_m}$ and on k_{+2} (25°C)	55
XV	60000 brain acetylcholinesterase form: Influence of pH and Ca^{2+} on the apparent $\underline{K_m}$ for acetylcholine hydrolysis	56
XVI	60000 brain acetylcholinesterase form: Influence of pH and Ca^{2+} on the derived $\underline{K_m}$ and on k_{+2} (25°C)	57
XVII	250000 molecular weight eel acetylcholinesterase form: pH dependence of the overall rate constant (k), acetylation rate constant (k_{+2}), and de-acetylation rate constant (k_{+3})	59
XVIII	250000 molecular weight eel AChE form: pH dependence of the ratios of reaction rate constants in the presence and absence of Ca^{2+}	60
XIX	250000 molecular weight eel acetylcholinesterase form: Thermodynamic activation parameters for acetylation in the presence and absence of Ca^{2+}	62
XX	250000 molecular weight eel AChE form: Thermodynamic activation parameters for de-acetylation in the presence and absence of Ca^{2+}	63
XXI	250000 molecular weight eel AChE form: Influence of pH and Ca^{2+} on the apparent $\underline{K_m}$	65
XXII	250000 molecular weight eel AChE form: Influence of pH and Ca^{2+} on the derived $\underline{K_m}$ and on k_{+2} (25°C)	66

LIST OF FIGURES

<u>Figure</u>	<u>Page</u>
1. Possible scheme for acetylcholine hydrolysis by acetylcholinesterase	7
2. Purification of ^3H -di-isopropylfluorophosphate by gel filtration	14
3. Binding of ^3H -di-isopropylfluorophosphate to chymotrypsin	15
4. Diagram of gradient gel electrophoresis of brain and eel acetylcholinesterase	18
5. Diagram of gradient gel electrophoresis of brain AChE forms separated by gel filtration	20
5a. Gradient gel electrophoresis of brain AChE forms	20a
6. Diagram of the collodion bag vacuum filtration system	24
7. Diagram of the pH-stat-titrimetric system	30
8. Representation of derived rate constants for acetylation and de-acetylation from the Arrhenius plots of eel acetylcholinesterase catalyzed acetylcholine hydrolysis	34
9. Representation of derived rate constants for acetylation and de-acetylation from the Arrhenius plots of brain acetylcholinesterase catalyzed acetylcholine hydrolysis	35
10. Reaction rate versus pH profiles of the 240000 molecular weight brain AChE catalyzed acetylcholine hydrolysis	45
11. Estimation of pK values associated with the 60000 molecular weight brain AChE catalyzed hydrolysis of acetylcholine	47
12. Analysis of pH versus rate profiles for acetylcholine hydrolysis catalyzed in the presence and absence of Ca^{2+} by eel AChE	61a
13. Ionic activation of eel AChE catalyzed acetylcholine hydrolysis	67
14. Gradient gel electrophoresis of brain AChE form B for 5 h and 9 h	70

LIST OF FIGURES (continued)

<u>Figure</u>	<u>Page</u>
15. Gradient gel electrophoresis of brain AChE form B for 15 h	71
16. Gradient gel electrophoresis of brain AChE form C for 5 h and 9 h	73
17. Gradient gel electrophoresis of brain AChE form C for 15 h	74

ABSTRACT

Three forms of brain acetylcholinesterase (AChE) were purified from bovine caudate-nucleus tissue and determined to have molecular weights of approximately 75000 (C), 240000 (B), and 330000 (A). by calibrated G-200 gel filtration. Gradient gel electrophoresis of AChE forms was also employed for molecular weight estimation. Using ^3H -di-isopropyl-fluorophosphate for labelling the active center of the enzyme, the forms of brain AChE were calculated to contain one (C), four (B), and six (A) active sites per molecule respectively. With a similar method, the 250000 molecular weight eel AChE form was determined to have two active centers.

Calcium activation of acetylcholine hydrolysis by bovine brain and eel AChE was analyzed in terms of changes in kinetic constants and thermodynamic activation parameters. De-acetylation was determined to be the rate-limiting step in acetylcholine hydrolysis by both 60000 and 240000 mol. wt. forms of the brain enzyme and 10 mM CaCl_2 increased the rate constant (k_{+3}) by 30% for both forms. For the smaller AChE form the effect of Ca^{2+} on de-acetylation was equivalent to its effect on the overall rate constant (k) and occurred without an effect on pK . In the case of the 240000 mol. wt. species, the overall rate constant was increased by Ca^{2+} by 33% at pH 8.0 and 81% at pH 7.25 and involved a pK shift of -0.2 pH units. For both brain enzyme forms the rate constants for acetylation (k_{+2}) were increased

by Ca^{2+} . Thermodynamic analysis suggested that Ca^{2+} activation of acetylation for both enzyme forms is entropically driven. Ca^{2+} effects on the apparent K_m and the Michaelis-Menten K_m were determined for each brain enzyme form. Differences between the two enzyme forms in terms of Ca^{2+} appears to result from association of low molecular weight species.

In the case of eel AChE, in the absence and presence of Ca^{2+} , both acetylation and de-acetylation contribute significantly to the overall velocity constant and both steps were enhanced by Ca^{2+} . Anomalous pK values were observed in the presence and absence of Ca^{2+} . These anomalous pK values were thought to occur due to the participation of both acetylation and de-acetylation in determining the overall velocity constant as well as the greater pH sensitivity of the acetylation step. Acceleration of acetylation and de-acetylation by Ca^{2+} occurred with a more favorable enthalpy of activation and a slightly less favorable entropy of activation. Effects mediated by Ca^{2+} on the apparent K_m and the Michaelis-Menten K_m were determined.

These effects of Ca^{2+} are discussed in terms of their possible significance in cholinergic neurotransmission as well as their possible basis in terms of the current kinetic and thermodynamic understanding of the serine proteases and esterases.

INTRODUCTION

History

The existence of the enzyme cholinesterase was suggested by Dale after it had been determined that acetylcholine was important in the function of the nervous system. Enzymes capable of hydrolyzing acetylcholine, thereby terminating its physiological action, were found initially in the blood. It was determined that both serum enzyme and enzyme from erythrocytes can hydrolyze choline esters at considerably faster rates than other esters (Vahlquist, 1935). In addition, a comparison of the hydrolytic pattern of different substrates indicated that the two enzyme sources contain enzymes of a different type. Serum cholinesterase hydrolyzes butyrylcholine two to three times more rapidly than acetylcholine; however, the erythrocyte enzyme hydrolyzes butyrylcholine extremely slowly (Nachmansohn & Rothenberg, 1944). In addition, whereas the red cell enzyme hydrolyzes the D-isomer of acetyl β -methylcholine rapidly (but not the L-isomer), neither isomer is hydrolyzed by the serum enzyme. (Glick, 1938; Hoskin & Trick, 1955). Also, erythrocyte enzyme shows substrate inhibition, whereas the enzyme from serum follows a pattern of increasing acetylcholine hydrolytic rate with increasing substrate concentration (Alles & Hawes, 1940). The enzyme from the red cell was named acetylcholinesterase by Marnay & Nachmansohn (1937).

Synaptic function

The significance of acetylcholinesterase in synaptic function relates to its role in terminating the action of the neurotransmitter acetylcholine. Much of the evidence supportive of this role has been obtained from experiments analyzing the actions of anti-cholinesterases on the end-plate action potential (e.p.p.) and miniature endplate potential (m.e.p.p.). Eccles & MacFarlane (1949) demonstrated that anti-cholinesterases slowed the time course and increased the relative size (voltage) of the slowly decaying component of the e.p.p. set up by single or repetitive nerve volleys. These agents, ranging from physostigmine to di-isopropylfluorophosphate, exerted their effects on the time course of the e.p.p. by inhibiting the neuro-muscular junctional acetylcholinesterase and as a consequence, slowing the removal of the active neurotransmitter acetylcholine. Acetylcholine is probably removed from the site of action in the synaptic cleft region by two mechanisms, enzymic hydrolysis and diffusion. In analysis of the acetylcholine release-receptor interaction process, Fatt & Katz (1952) found that in the absence of an anti-cholinesterase, the effect of acetylcholine (recorded in the form of external m.e.p.p) declines with a half time of about 1.0-1.5 msec (frog muscle, 20° -25° C). This value was of the same order as the estimated open time of the elementary ion gates affected by acetylcholine molecules (Katz & Miledi, 1971, 1972). However, after treatment with a cholinesterase inhibitor, diffusion and receptor binding would be major factors in determining the time course of the cholinergic response, and

conductance change became much longer (Fatt & Katz, 1952; del Castillo & Katz, 1956; Katz & Miledi, 1965).

In order to determine whether the prolongation of the time course of the quantal conductance change was more likely due to effects on acetylcholinesterase, rather than actions on the acetylcholine receptor, Katz & Miledi (1972, 1973) analyzed the statistical nature of the acetylcholine potential and its molecular components. In these studies on "acetylcholine noise" the effect of prostigmine on the time course of the transmitter actions was evaluated. Results of these investigations showed that prostigmine had little or no effect on the duration of the receptor processes responsible for the post-synaptic conductance increase, while greatly prolonging the duration of the overall post-synaptic event.

Synaptic geometry and synaptic localization of acetylcholinesterase are other factors which may be significant in describing the basis for observed time courses of cholinergic events (Eccles & Jaeger, 1958) ; Porter & Barnard (1975). Porter and Barnard (1975) have shown, using the techniques of radioautography, that the acetylcholine receptor and acetylcholinesterase are not localized at the same synaptic regions. Although detailed information is lacking concerning the effect of partial acetylcholinesterase inhibition on the above synaptic neurotransmission parameters, it may be that changes in the activity of the enzyme could alter the time course of synaptic events occurring subsequent to acetylcholine release. Such changes in enzyme activity require consideration of possible enzyme activators in addition to inhibitors. In order

to consider the possible basis of modification of enzyme activity, it is necessary to describe briefly certain features of the enzyme active center.

The enzyme active site is considered to include two subsites. One, an anionic site, is thought to confer substrate specificity and the other, the esteratic site, mediates the hydrolytic process (Wilson & Bergman, 1950a, 1950b; Wilson, 1952; Bergmann et al., 1950; Wilson et al., 1950). Analysis of pH vs. rate profiles of acetylcholinesterase catalyzed reactions suggested the existence of two pK's, one having a value of approximately 6.7 and a second with a value of about 9.5. This observation led to the suggestion that there were two essential ionizable groups at the esteratic site. These two groups, essential to the esteratic process, may be the imidazole of histidine and the hydroxyl moiety of serine. The involvement of serine is suggested by the identification of serine phosphates in hydrolysates following enzyme labelling with organophosphorous compounds. It appears that the reactive serine acts as a nucleophile in the attack of the carbonyl carbon of the substrate acetylcholine. The involvement of histidine is suggested both by the pK value and the identification of the essential histidine-57 associated with serine-195 at the active center of chymotrypsin, a serine protease with a catalytic mechanism that may be analogous to that of acetylcholinesterase.

Possible enzyme regulatory sites

There have been suggestions that anionic sites distinct from the primary, substrate-binding, anionic site exist and may regulate

activity at the esteratic or catalytic site (Changeux, 1966). Ligands such as gallamine triethiodide were found to reverse the enzyme inhibition due to decamethonium. Generally, it has been found that under certain conditions, the catalytic activity of acetylcholinesterase can be modified by ionic-non-covalent ligand binding at sites other than the catalytic site. As a consequence, the enzyme meets this major criterion for allosteric control (Monod et al., 1965; Changeux, 1966; Kitz et al., 1970; Roufogalis & Quist, 1972; Belleau et al., 1970; Taylor & Lappi, 1975). A general finding has been that divalent cations (Ca^{2+} , Mg^{2+} , Ba^{2+}) can exert an acceleratory effect on the rate of hydrolysis of a number of substrates catalyzed by acetylcholinesterases.

Ca^{2+} is of particular interest in that it has been implicated in various aspects of cholinergic neurotransmission. It has been suggested that Ca^{2+} plays a central role in both presynaptic neuronal membrane excitation-transmitter release coupling (Katz & Miledi, 1965b). Influx of Ca^{2+} following pre-synaptic membrane depolarization seems to be essential for subsequent neurotransmitter release. The mechanism by which Ca^{2+} exerts this effect has not been determined. In addition, the time course of neurotransmitter-receptor mediated post-synaptic membrane conductance changes may be influenced by Ca^{2+} (Changeux et al., 1969). Of principal interest in the present studies is acceleration of acetylcholine hydrolysis (a maximum of approximately a two-fold) by electric eel and mammalian brain acetylcholinesterase by CaCl_2 . The mechanism of Ca^{2+} acceleration of acetylcholine hydrolysis catalyzed by acetylcholinesterases

is not known; however, In the present study, analyses of thermodynamic activation parameters and other kinetic constants of brain and eel acetylcholinesterase catalyzed hydrolysis of acetylcholine have been employed to examine possible mechanisms of Ca^{2+} activation of the enzyme.

Thermodynamic and kinetic approaches

Evaluation of thermodynamic activation parameters and kinetic constants has proved useful in analysis of ionic effects on several enzyme systems. For example, Kayne & Swelter (1965) studied thermodynamic parameters in describing the activating effect of K^+ and Mn^{2+} on pyruvate kinase and found that the "activated" enzyme in contrast to the "unactivated" form had a different energy of activation. Inhibition of acetylation, accounting for the inhibitory effect of F^- on acetylcholinesterase catalytic rate, was deduced in part from analysis of activation energy (Heilbronn, 1965). The two step, acetylation-deacetylation catalytic process of acetylcholinesterase (Wilson & Bergman, 1950; Wilson *et al.*, 1950) shown in Figure 1 is also shared by trypsin and chymotrypsin (Kaufman *et al.*, 1949; Butler, 1941). Studies in these systems have utilized activation parameter analysis to determine the rate determining step as a function of substrate used (Snoke & Neurath, 1956). These methods, therefore, appear applicable to the characterization of the reaction steps that may be influenced by ionic rate modifiers. Furthermore, some indication of the nature of active site groups may be revealed by studies of the effect of pH on

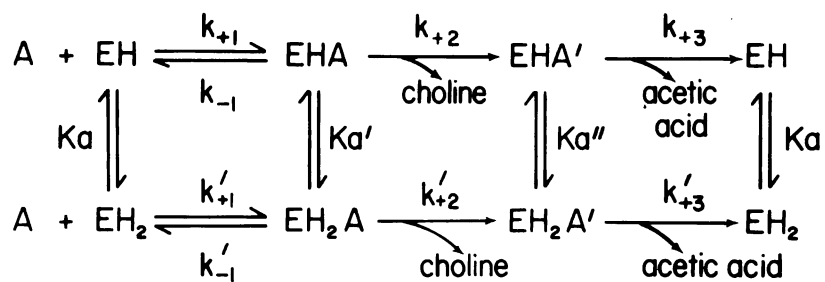
SCHEME I

Figure 1: Possible scheme for acetylcholine hydrolysis by acetylcholinesterase. Abbreviations used are: A is the substrate acetylcholine; EH is the active form of the enzyme; EH_2 is the protonated free enzyme; EHA and $EH_2 A$ are the acetylated forms; the k's refer to the rate constants in the indicated directions; Ka, Ka', and Ka'' refer to the respective ionization constants.

catalytic rate constants and on the K_m . The nature of the temperature dependence of the rate constants, measured at different pH values, may reveal processes such as temperature effects on the equilibrium between two forms of the enzyme, as is seen for trypsin (Gutfreund, 1972) or provide information as to enthalpy and entropy of activation changes accompanying changes in ionization of reaction intermediates. With trypsin, higher energies of activation at lower pH values (pH 6.0) compared to higher pH's (pH 8.0) suggested two forms of the enzyme, one predominating at the lower pH's suggesting one ionization state, and a second at higher pH's suggesting a different ionization form. Some aspects, including active site numbers, of the molecular weight forms of brain acetylcholinesterase and eel acetylcholinesterase were studied as preparatory for and contributory to the analysis of the Ca^{2+} acceleration phenomenon.

Active site determinations on forms of mammalian brain and eel acetylcholinesterase

Early attempts to isolate and subsequently purify the mammalian brain AChE proceeded with some difficulty due to problems in solubilizing the enzyme. This difficulty was presumed to reflect strong association with membrane constituents of brain tissue. Some investigators utilized detergents to solubilize the enzyme (Ord and Thompson, 1951; Jackson and Aprison, 1966; Kremzner *et al.*, 1967; Ho and Ellman, 1969; Shirachi *et al.*, 1970). Other approaches involved the use of proteases (Ho and Ellman, 1969), acetone (Lawler, 1964), butanol (Jackson and Aprison, 1966b) and the serine protease, elastase (Kaplay and Jagannathan, 1966; 1970). Mammalian brain

acetylcholinesterase used in this study was isolated from bovine caudate-nucleus tissue by a method described by Chan et al., (1972). This method is based upon a relatively simple procedure of homogenization and centrifugation in 0.32 M sucrose containing 1 mM EDTA and is in contrast to the previous methodology. The use of the EDTA-sucrose method seems to be less severe and the ready solubilization with EDTA suggests that the association of the enzyme with the membrane may not be as tight as previously supposed and also may involve di-valent cations (Chan et al., 1976). In considering the results from many of the above approaches, the brain enzyme has been shown to exist in multiple forms which has been characterized in terms of molecular weight, inhibitor sensitivity and glycoprotein nature (Chan et al., 1972; Gardner et al., 1975). It has been suggested that the existence of multiple forms may be due to association of a lowmolecular weight form (Hollunger & Niklasson, 1973; McIntosh & Plummer, 1973; Adamson et al., 1975). The thermodynamic and kinetic analyses described above require accurate knowledge of catalytic-site concentrations. This determination was accomplished in the present study by labelling brain and eel acetylcholinesterase forms with radioactive di-isopropyl-fluorophosphate. Determinations of eel AChE active site concentration was performed both for purposes of comparison with brain AChE forms and to resolve the controversy about the precise active-site number for the 250000 molecular weight form of this enzyme (Froede & Wilson, 1970; Leuzinger, 1971).

Questions considered in this study:

- 1) Do the multiple molecular forms of brain acetylcholinesterase possess identical active site numbers or are the active site numbers multiples of one another, suggestive of an association of acetylcholinesterase forms as in an aggregation process?
- 2) Using the same method, radioactive di-isopropylfluorophosphate labelling, applied to the brain active site question, do results support two or four active sites for the Sigma eel 250000 molecular weight form? Both active site numbers have been claimed in the literature.
- 3) Does the presence of Ca^{2+} accelerate the hydrolysis of acetylcholine catalyzed by brain acetylcholinesterase?
- 4) Are there differences in the nature of the Ca^{2+} effect depending upon which brain acetylcholinesterase form is examined?
- 5) What are the effects of Ca^{2+} on the acetylation and de-acetylation rate constants of brain acetylcholinesterase?
6. What are the effects of Ca^{2+} on the acetylation and de-acetylation rate constants of eel acetylcholinesterase?
7. How does pH influence the Ca^{2+} effects on the rate constants for brain and eel acetylcholinesterase?
8. What are the thermodynamic activation parameters that describe the Ca^{2+} effects on the rate constants and what might be tentative conclusions drawn from these effects?
9. What are the influences of Ca^{2+} on the apparent and derived K_m and how might these effects be explained?
10. What are the effects of Ca^{2+} on the apparent reaction pK for brain and eel acetylcholinesterase catalyzed acetylcholine hydrolysis? How might they be explained?
11. What conclusions can be drawn from gradient gel electrophoresis concerning the possible existence of brain acetylcholinesterase isoenzymes?
12. What are the limitations to interpretations that must be considered in beginning to answer the above questions?

METHODS

Materials

General chemicals used were analytical-reagent grade. Acetylthiocholine iodide, pyridine 2-aldoxime iodide, acetylcholinesterase (acetylcholine hydrolase, EC 3.1.1.7.; type III, electric eel) and chymotrypsin (type I, bovine pancreas) were obtained from Sigma Chemical Co., St. Louis, MO. Bovine brains were obtained from a local slaughterhouse. Di-isopropyl fluorophosphate (99% pure) was from Aldrich Chemical Co., Milwaukee, WI., and ^3H di-isopropylfluorophosphate (0.87 Ci mmol) was from New England Nuclear Corp., Boston, MA. Gel-calibration proteins were products of Boehringer Mannheim Corp., San Francisco, CA. Gelatine (U.S.P.) was obtained from Braun-Knecht-Heimann, San Francisco, CA. Ethylene diamine tetraacetic acid (tetra sodium salt) was obtained from Aldrich Chemical Co., Milwaukee, WI. Other more common laboratory reagents were also obtained from the above suppliers.

Sephadex G-10 and G-200 materials were obtained from Pharmacia Fine Chemicals, Piscataway, NJ, U.S.A., and the collodion bags (8 ml capacity) were from Schleicher and Schuell, Keene, NH, U.S.A.

I.

Active Site Determinations

Preparation of bovine brain and eel acetylcholinesterase forms

Acetylcholinesterase forms were purified from bovine caudate-nucleus tissue by the method of Chan et al. (1972). The procedure involved

solubilization in 0.32M-sucrose containing 1 mM EDTA then fractionation of the soluble material with $(\text{NH}_4)_2\text{SO}_4$. This was followed by affinity chromatography using m-trimethylammonium aniline as the affinity ligand and by a separation of three forms of acetylcholinesterase by Sephadex G-200 chromatography. These procedures are taken from Chan et al. (1972). The Sephadex G-200 column had been equilibrated with and the samples eluted in 30 mM Tris-HCl buffer, pH 7. The specific activities of each acetylcholinesterase form were determined to be 450-500 mmol of acetylthiocholine hydrolyzed/h per mg of protein by the procedure of Ellman et al. (1961) and their homogeneity was verified by polyacrylamide-gel electrophoresis (Gardner, 1974). For routine experiments, the limited stability of such highly purified forms was counteracted by the addition of small quantities of the less-pure $(\text{NH}_4)_2\text{SO}_4$ precipitate of brain acetylcholinesterase (Chan et al., 1972). This procedure introduced approximately 5% additional enzyme protein to the purified proteins, which was taken into account in subsequent calculations of active site numbers. For determinations of the active site concentration of AChE derived from electric eel tissue, the commercial preparation obtained from Sigma (type III) was used without further purification. The determination of precise concentrations of acetylcholinesterase used in labelling experiments involved comparison of observed activity with the known activity of purified forms of the enzyme (Chan et al., 1972). This method was accurate to within 3% in our hands when the enzyme activity was correlated with protein concentration determined by the fluorescamine protein assay procedure described

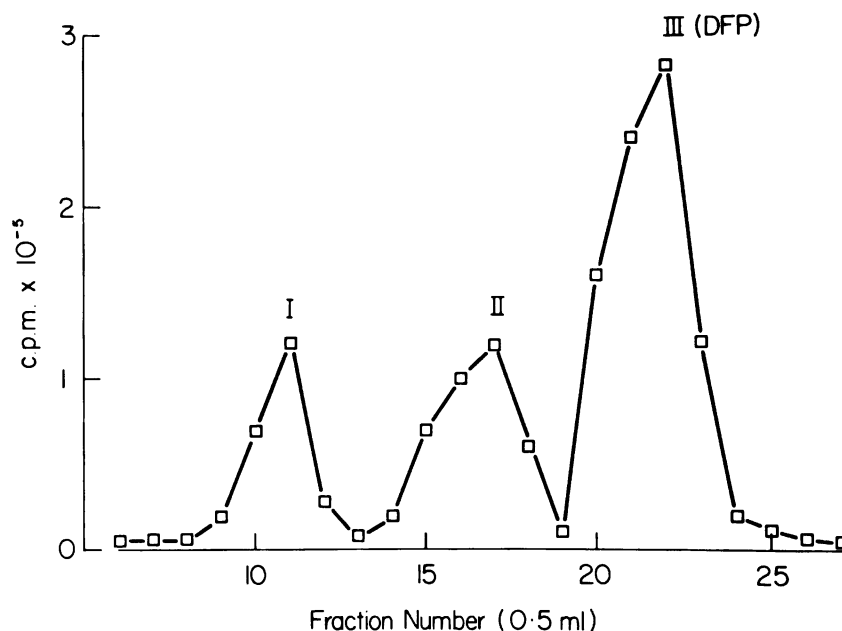
by (Bohlen et al., 1973).

3

Purification of ³H di-isopropylfluorophosphate

In initial studies unexpectedly low active site concentrations suggested possibly incorrect specific activity of the active site label ³H di-isopropylfluorophosphate. Since accurate determination of the enzyme catalytic site concentration necessitated a precise determination of the specific radioactivity of ³H di-isopropylfluorophosphate, the removal of radioactive impurities from commercial preparations was required. This was done by gel filtration on columns (0.8 cm x 56 cm) of Sephadex G-10 equilibrated with and eluted with distilled water (Figure 2). Radioactive peaks I (void volume) and II lacked acetylcholinesterase inhibitory activity, whereas peak III contained over 95% of the inhibitory activity of the commercial preparations (Figure 2). To determine the relative homogeneity of the radioactive species in peak III, the material was incubated with an estimated 30 fold excess of chymotrypsin (0.5 μ M) for 60 min at 21° C. This enzyme is a serine protease containing one site per molecule that can be phosphorylated by di-isopropyl-fluorophosphate. On gel filtration of the incubation mixture all the radioactivity appeared in the void volume in association with the enzyme protein (Figure 3). Thus all of the radioactive material in peak III appeared to be due to a phosphorylating agent, presumably di-isopropylfluorophosphate.

Determination of the radioactivity of samples were made in Aquasol (New England Nuclear Corp.) in a Beckman model LS 100 liquid-scintillation counter. With the preset ³H window module, counting efficiency was 36%. Since it was possible that the radioactive



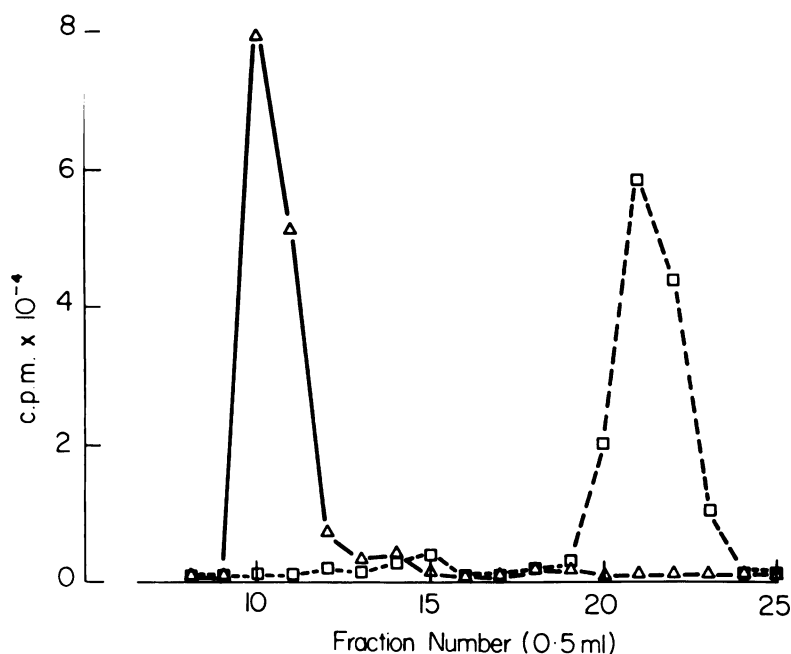
3

Figure 2: Purification of ³H-di-isopropylfluorophosphate by gel

filtration. Commercial preparations of ³H-di-isopropylfluorophosphate were chromatographed on a column (0.8 cm x 56 cm) of Sephadex G-10. On elution with water, fractions (0.5 ml) were collected for measurement of radioactivity and acetylcholinesterase inhibitor activity. Radioactivity peaks I in the void volume (fractions 9-12) and II (fractions 14-18) lacked enzyme inhibitory activity. Peak III (fractions 19-24) contained over 95% of the acetylcholinesterase inhibitory activity of the

3

commercial preparation and was presumed to be ³H-di-isopropyl-fluorophosphate.



3
Figure 3: Binding of ³H-di-isopropylfluorophosphate to chymotrypsin.

3

H-di-isopropylfluorophosphate was separated from radioactive impurities present in the commercial preparation by gel filtration and re-applied to a column (0.8 cm x 56 cm) of Sephadex G-10. On elution with water, fractions (0.5 ml) were collected for measurement of radioactivity

3

and the ³H-di-isopropylfluorophosphate was separated as a peak of

3

material between fractions 19-24 (---). When ³H-di-isopropylfluorophosphate was incubated with a 30-fold excess of chymotrypsin at 21° C for 1 h, all radioactivity appeared in the void volume (fractions 9-12) in association with enzyme protein (—)

impurities present in the commercial preparations of H^3 -di-isopropylfluorophosphate could be degradation products, the concentration of di-isopropylfluorophosphate was measured. This was done by comparison of the rates of inhibition of eel acetylcholinesterase with unlabelled di-isopropylfluorophosphate ($3.3\mu\text{M}$) and H^3 -di-isopropylfluorophosphate at the same apparent concentration indicated to be present by the estimate of the manufacturer. The procedure involved the determination of bimolecular rate constants from equations of the form:

$$k_i = \frac{2.303 \log (v_1 / v_2)}{(t_2 - t_1) (i)}$$

where v_1 and v_2 are the measured velocities of substrate reactions catalyzed by the esterase remaining uninhibited at times t_1 and t_2 of the reaction, i is the inhibitor concentration and k_i is the reaction velocity constant (Aldridge, 1950; Hartley & Kilby, 1952). The average value of k_i from three determinations was $1.73 \times 10^{-4} \text{ M}^{-1} \text{ min}^{-1}$ and $1.81 \times 10^{-4} \text{ M}^{-1} \text{ min}^{-1}$ for di-isopropylfluorophosphate and H^3 di-isopropylfluorophosphate respectively. Several time points (3 min to 15 min) were examined to confirm linearity of the inhibition reaction. Since the difference between these values represented only 4% of the expected value, the quantity of H^3 di-isopropylfluorophosphate stated to be present in the commercial preparation was considered to be accurate.

Gradient gel electrophoresis of acetylcholinesterase forms

As indicated previously (Chan et al., 1972), calibrated molecular-

sieve chromatography was used to estimate the approximate molecular weights of bovine brain acetylcholinesterase forms. This method demonstrated three major forms (A, B, C) with apparent molecular weights of 330000, 230000, and 75000 respectively (Chan et al., 1976). Independent estimations of the molecular weights of different acetylcholinesterase forms were made by using polyacrylamide-gradient-gel electrophoresis, with calibration by marker proteins of established molecular weights (in parentheses), including aldolase (158000), catalase (240000), ferritin (540000), ovalbumin (45000), and bovine serum albumin (67000). These markers, (10 -150 μ g of protein) and acetylcholinesterase samples (2-20 μ g of protein) were applied to precast gradient gels (type PAA4/30) Pharmacia Fine Chemicals, Uppsala, Sweden). Electrophoresis was carried out in the Pharmacia model GE4 apparatus at 125V (constant voltage) for 15 h in a buffer system containing 81.5 mM-boric acid, 89 mM-Tris base and 2.68 mM-disodium EDTA at pH 8.3. Control experiments established that 15 h electrophoresis time represented equilibrium conditions. The gels were then separated into two halves one of which was fixed in 10% (w/v) trichloroacetic acid then stained for protein with 1% (w/v) Comassie Blue, and the other stained for acetylcholinesterase activity by the procedure of Uriel (1963).

Results

Figure 4 shows the electrophoretic profile of a semi-purified bovine brain and eel acetylcholinesterase preparation before the separation of forms by gel filtration (Chan et al., 1972). For the brain, multiple enzyme-staining bands were noted, three of which

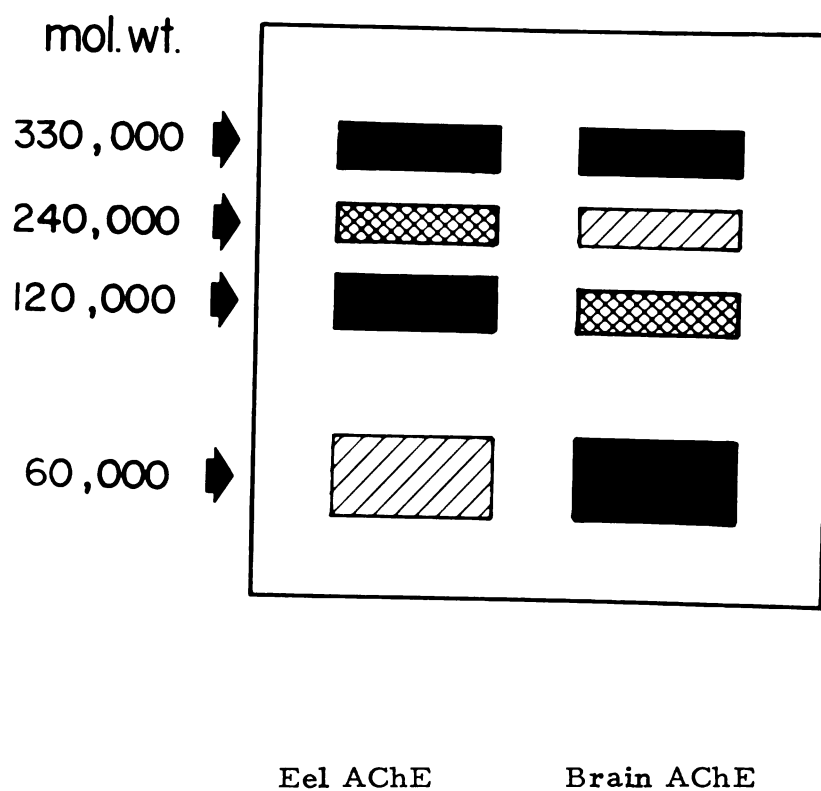


Figure 4: Diagram of gradient gel electrophoresis of brain and eel acetylcholinesterase. Bovine brain and electric eel acetylcholinesterase were obtained as described in Methods and applied to gradient polyacrylamide gels (82 mm width x 76 mm length) for electrophoresis at 125 V for 15 h. The gels were then stained to reveal AChE activity. Band migration of the 330000- and 60000-molecular weight enzyme forms was approximately 32 and 60 mm from the origin respectively. Intensity of coloring corresponds to the intensity of enzyme activity.

(A, B, and C) had molecular weights of 330000, 240000, and 60000, which may correspond to the forms separated on Sephadex G-200 columns. Other acetylcholinesterase-staining bands were also present, in particular, one representing an enzyme form of approximately 120000. To examine if such acetylcholinesterase forms originate from the electrophoretic procedure, forms A, B, and C of the brain enzyme were separated by gel filtration and then applied individually to the gradient gels for electrophoresis. As shown in Figure 5, form A on the gradient gel is characterized by a molecular weight estimate very similar to that observed on G-200, suggesting no change of molecular weight upon electrophoresis. However, the application of form B resulted in the appearance of a major active acetylcholinesterase species of molecular weight of 120000. The sample containing primarily form B also contained a small quantity of form A, as shown in the gradient gel enzyme-staining profile. Application of form C (75000 molecular weight by G-200) resulted in a single form of molecular weight 60000. In order to resolve the apparent discrepancy regarding the molecular weights of form B measured by G-200 chromatography or gradient gel electrophoresis time course experiments were performed. In these experiments, forms B and C from G-200 were run for varying (pre-equilibrium) times as well as to equilibrium. The results of these experiments, since they are not related to active site estimates, are reported in a later section (see page 69)

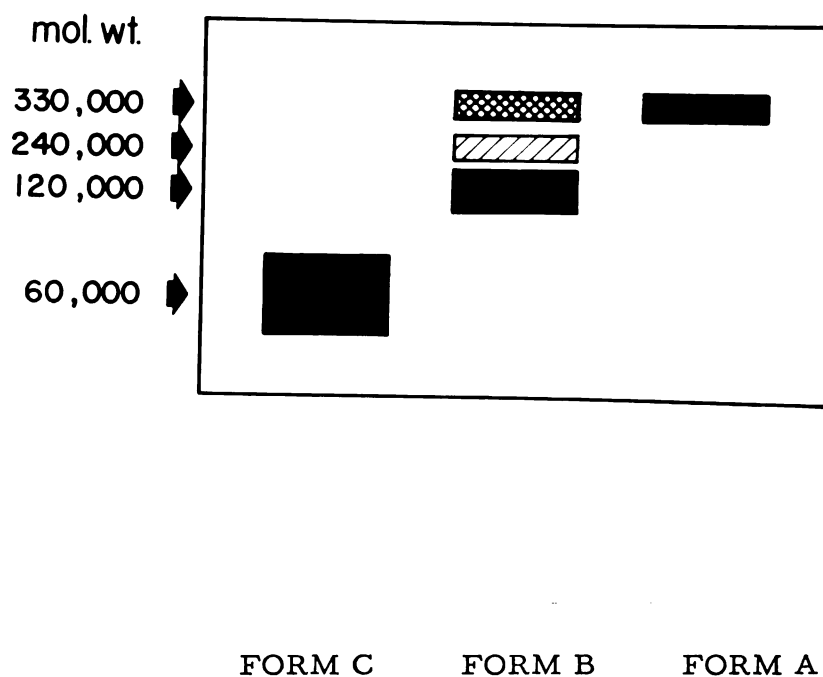


Figure 5: Diagram of gradient-gel electrophoresis of brain AChE forms separated by gel filtration. Bovine brain AChE was purified and separated into three forms of different molecular weight by gel filtration on Sephadex G-200 as indicated in Methods. The forms were then applied individually to gradient polyacrylamide gels (82 mm width x 76 mm length) for electrophoresis at 125 V for 15 h. The gels were then stained to reveal AChE activity. For reference the migration of the 330000- and 60000-molecular weight AChE forms was approximately 32 and 60 mm from the origin respectively. Intensity of coloring corresponds to the intensity of enzyme stain.

--330000 mol. wt.

--120000 mol.wt.

---- 60000 mol.wt.

Form C Form B Form C

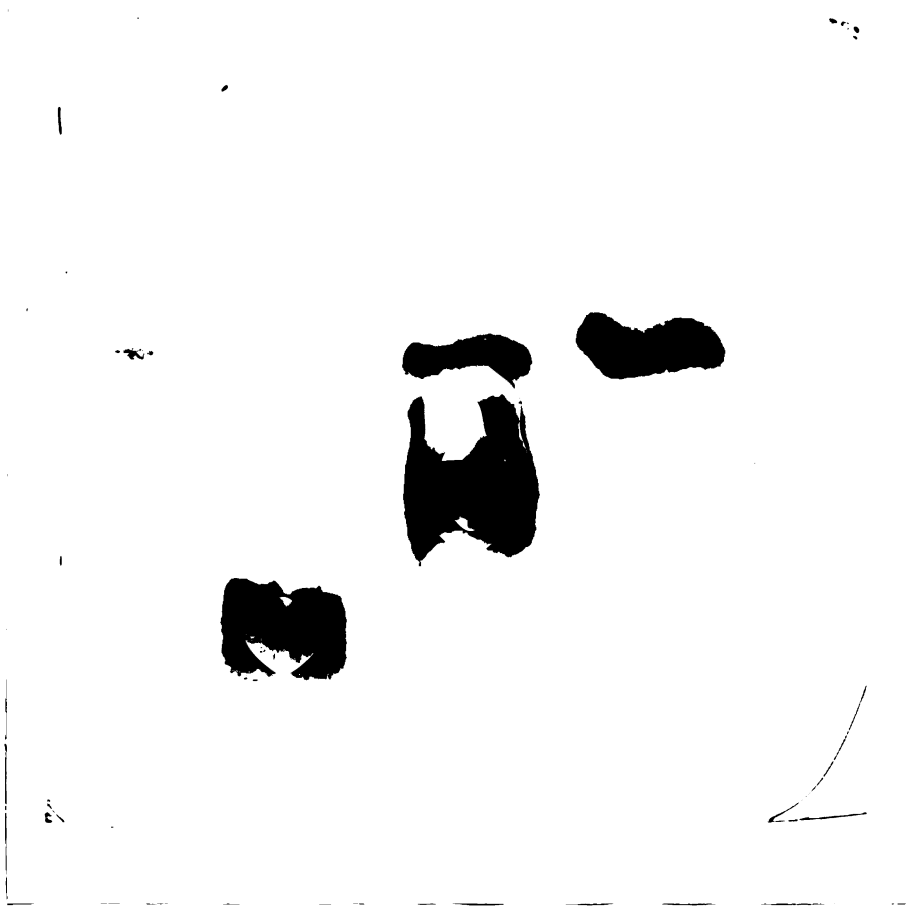
**Figure 5a: Gradient gel electrophoresis of brain AChE forms
(see Figure 5 for legend)**

--- 0.000 mol wt.
-- 1.000 mol wt.
- 2.000 mol wt.

Form C Form B Form A

Figure 2a: Gradient of electrophoresis of brain AChE forms

(see Figure 2 for legend)



³

Phosphorylation of acetylcholinesterase forms by ³H di-isopropyl-fluorophosphate

The phosphorylation of acetylcholinesterase preparations was carried out in 30 mM-sodium phosphate buffer, pH 8.0 at 2-4° C for approximately 30 min. Enzyme concentration was varied between

0.5 and 20 µg in a reaction volume of 0.1 ml and the range of

³

H di-isopropylfluorophosphate concentration was from 5 to 50µM.

Non-specific phosphorylation was minimized by monitoring enzyme activity such that the reaction was terminated by (10-fold) dilution with 30 mM-sodium phosphate buffer when 98% inhibition of enzyme activity had been produced (approximately 30 min). The mixture was

then applied to a Sephadex G-10 column in the same manner

as that used for di-isopropylfluorophosphate purification (Figure 2) and

eluted with 30 mM-sodium phosphate buffer containing 200 mM NaCl.

The flow rate was 4.3 ml/h. The phosphorylated enzyme separated in

the void volume (peak I, fractions, 9-12) whereas unchanged ³H di-isopropylfluorophosphate appeared in fractions 19-24 (peak III).

Fractions 15-18 also contained radioactive material (peak II),

presumed to be di-isopropylphosphate ion. Specificity of ³H di-

isopropylfluorophosphate labelling was determined by using pyridine

2-aldoxime, a reactivator of phosphorylated acetylcholinesterase,

as illustrated for the eel enzyme in Table I. The presence of

2.3 mM pyridine-2-aldoxime in the reaction mixture decreased

the radioactivity present in peak I of the Sephadex G-10 column

separation to less than 5% of control values. When pyridine-2-aldoxime

(2.3 mM) was added after phosphorylation, and the reaction mixture

monitored for enzyme activity to the point of complete re-activation,

Table I

3
Effects of pyridine-2-aldoxime on ³H-di-isopropylfluorophosphate
labelling of eel acetylcholinesterase

Total radioactivity in fractions from Sephadex
G-10 chromatography (C. P. M.)

conditions	Peak I	Peak II	Peak III
control	8200 ± 450	6050 ± 350	5160 ± 430
pyridine-2-aldoxime present <u>during</u> in- cubation	400 ± 210	4800 ± 320	20000 ± 850
pyridine-2-aldoxime added <u>after</u> in- cubation	100 ± 80	17700 ± 750	3400 ± 320

Eel acetylcholinesterase (2µg of enzyme protein) was incubated with
³
50 µM ³H-di-isopropylfluorophosphate (20000-25000 c. p. m.) in
30 mM phosphate buffer, pH 8.0 at 2-4° C. Labelling was terminated
by dilution (10 fold) with buffer when enzyme activity was inhibited by
98% and the mixture was separated on a Sephadex G-10 column.

Peak I represents the enzyme protein that was eluted in the

3

void volume, whereas Peaks II and III may represent ³H-di-isopropyl-
³
phosphate and unchanged ³H-di-isopropylfluorophosphate.

less than 2% of the radioactivity appeared in the fraction containing enzyme protein. The increase of radioactivity in peak II, which occurred on the addition of pyridine-2-aldoxime after phosphorylation, suggests that such fractions contain di-isopropyl phosphate. Similar experiments were carried out with different forms of brain acetylcholinesterase and in all cases ³H di-isopropylfluorophosphate labelling was greater than 95% reversible by pyridine-2-aldoxime, suggesting a minor degree of phosphorylation to non-specific sites.

Two other methods were used for the separation of unchanged ³H di-isopropylfluorophosphate from radioactively labelled enzyme to test the validity of the gel-filtration procedure. In Method 1, collodion bag vacuum filtration at 4° C, involved placing samples of the reaction mixture (0.1 ml) with 5 ml of the sodium phosphate buffer into 8 ml-capacity collodion bags (molecular weight greater than 40000 retained). The bags were slipped into a glass tube open to the atmosphere and then inserted into a larger glass chamber attached to the laboratory vacuum line. (See Figure 6). After vacuum filtration to a volume 0.3 ml (80 min), an additional 5 ml of the phosphate buffer was added and the procedure repeated a third time. This method removed excess ³H di-isopropylfluorophosphate within 4 h of enzyme phosphorylation and the final volume of 0.3 ml was shown by control experiments to contain no free ³H-di-isopropylfluorophosphate. Method 2 was dialysis of the reaction mixture against water for 36h. Over this time-period phosphorylated cholinesterases by the release of an alkyl or alkoxy moiety in a first order reaction (Hobbiger, 1955; Harris et al., 1966) may be converted to forms that are not reactivated by pyridine-2-aldoxime.

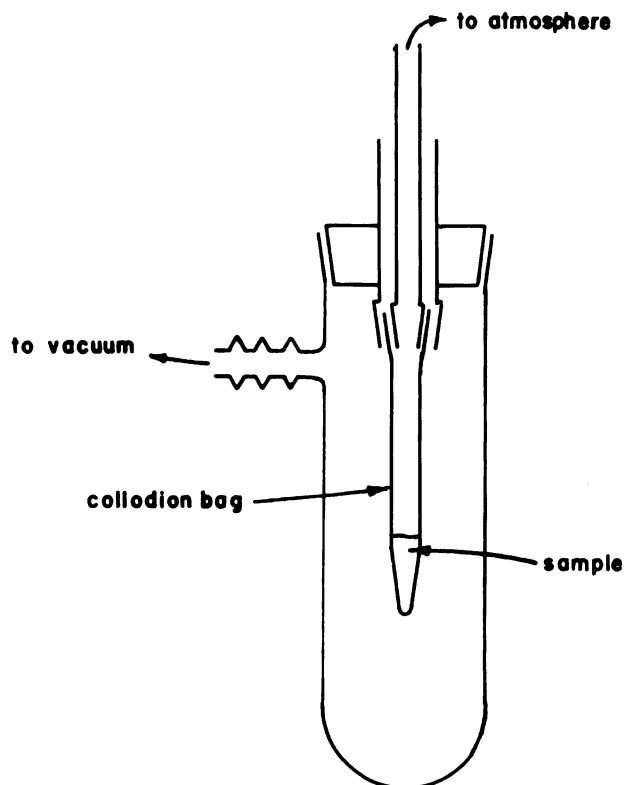


Figure 6: Diagram of the collodion bag vacuum filtration
3
system used for removal of unreacted H-di-isopropylfluorophosphate
in the active site studies as well as for protein concentration in the
ion activation studies.

3

In the case of the ^3H di-isopropylphosphorylated enzyme this "aging" process could result in the loss of 50% of the radioactivity of the labelled molecule. To measure the extent of this process the kinetics of "aging" were estimated by two methods. The first involved estimation of the degree of re-activation by pyridine 2-aldoxime as a function of time from phosphorylation, and the second method involved measurement of the loss of radioactivity from the ^3H -di-isopropylphosphorylated enzyme complex with time. The results of such experiments permitted computation of an estimated correction factor to approximate the original ^3H di-isopropylfluorophosphate labelling of the enzyme protein.

Active-site number for acetylcholinesterase forms

As pointed out in the the Introduction, the value of the rate constants can be estimated only from knowledge of the numbers of active sites associated with each enzyme species. In this section the active site determinations are presented to provide a basis for the computations of the rate constants which follow.

For the determination of the active-site number of eel electric-tissue acetylcholinesterase, the enzyme form that separated on Sephadex G-200 chromatography with a molecular weight of 250000 was used. The separation of unchanged ^3H di-isopropylfluorophosphate from labelled enzyme protein was carried out by G-10 column-chromatographic, vacuum-filtration, or dialysis procedures. Table II shows that by each method, eel acetylcholinesterase contained approximately two active sites per molecule of molecular weight 250000. In

Table II

ACTIVE-SITE NUMBERS OF ACETYLCHOLINESTERASE FROM
EEL ELECTRIC TISSUE

Separation method	No. of determinations	Enzyme protein (μ g)	Number of Active sites per molecule
Dialysis	7	1-20	1.85 \pm 0.11
Vacuum filtration	16	5-6.5	2.19 \pm 0.10
Gel filtration	5	6.5	2.26 \pm 0.26

Electric eel AChE (1-2 μ g) was labelled with ^3H di-isopropylfluorophosphate under conditions described in the Methods section. Labelled enzyme protein was separated from unchanged ^3H di-isopropylfluorophosphate by three methods: dialysis for 36 h, collodion-bag vacuum filtration or gel-filtration on Sephadex G-10. Number of active sites per molecule was calculated on the basis of a molecular weight of the enzyme of 250000 with appropriate corrections for non-specific phosphorylation, and also for the dialysis procedure, the process of "aging". Active site numbers represent mean values \pm S. E. M.

the case of bovine caudate-nucleus tissue acetylcholinesterase forms, the Sephadex G-10 chromatographic method for separation of unchanged

³H di-isopropylfluorophosphate was used exclusively. Table III shows that the brain acetylcholinesterase forms A, B, and C were estimated to contain approximately six, four, and one active sites per molecule respectively.

Table III

ACTIVE-SITE NUMBERS OF BRAIN ACETYLCHOLINESTERASE FORMS

AChE form	No. of determinations	Molecular weight	Enzyme protein (μ g)	Active-site number per molecule
A	4	330000 (F) 310000 (E)	1.19	5.88 \pm 0.16 5.52 \pm 0.15
B	5	230000 (F) 120000 (E)	0.6- 7.5	3.64 \pm 0.11 1.98 \pm 0.12
C	4	75000 (F) 60000 (E)	0.49-3.0	0.82 \pm 0.12 1.05 \pm 0.13

Brain acetylcholinesterase forms were separated as detailed in Methods and labelled with ^3H di-isopropylfluorophosphate. The labelled enzyme protein was separated from unchanged ^3H -di-isopropylfluorophosphate by gel filtration on Sephadex G-10. Active-site numbers per molecule were calculated on the basis of the molecular weights given, with appropriate corrections for non-specific phosphorylation. The estimates of molecular weights of individual AChE forms were made by gel filtration (F) on Sephadex G-200 and by gradient-gel electrophoresis (E). Active-site numbers represent mean values \pm S. E. M.

II

Ion Activation of Acetylcholinesterase

The preparation of brain acetylcholinesterase forms was performed as described earlier except that to obtain sufficiently high enzyme activities for the kinetic experiments, the G-200 fractions associated with the different molecular weight forms were concentrated using collodion bag filtration at 4° C. The degree of concentration required was determined by the initial enzyme activity associated with the pooled G-200 fractions for each form but generally was four-fold. The determination of precise concentrations of each enzyme form used in the kinetic experiments was performed as described earlier for determinations of the enzyme concentration employed in the active site studies.

Kinetic measurements

Kinetic measurements was based upon titration of protons released with acetylcholine hydrolysis, using a Radiometer automatic titrator (TTT1C) and Titrigraph (SBR2C). This procedure is based upon measuring the rate of addition of sodium hydroxide required to maintain a pre-set pH. As the enzyme-catalyzed acetylcholine hydrolysis proceeds the reaction solution becomes more acidic. A pH change occurs as a consequence of the dissociation of acetic acid, the second reaction product. Since within the pH range of these experiments, the rate of appearance of protons is equal to the rate of acetylcholine hydrolysis, a measure of the rate of NaOH addition necessary to maintain a constant pH should equal the rate

of acetylcholine hydrolysis. A Radiometer G-202C glass hydrogen ion electrode and a Beckman 40249 Ag/AgCl reference electrode were employed for pH measurement. In addition, a Radiometer T-301 continuous temperature compensation electrode was used throughout. Dual calibrated glass syringes allowed simultaneous additions of the 5 mM NaOH titrant (CO_2 -free) as well as 5 mM acetylcholine to replace hydrolyzed substrate. Concomitant with the syringe drive delivering titrant and substrate, a common mechanical linkage drives a pen which graphs volume of titrant delivered (Y-axis) per unit time (X-axis). This volume of titrant is specified by volume calibration of the syringes with water in order to determine the volume of titrant and substrate solution displaced per unit of distance on the Y-axis (see Figure 7) The same pair of syringes were utilized throughout the experimental series. The 100 ml reaction volume was contained in a 125 ml capacity water-jacketed reaction vessel. A slow stream of N_2 covering the surface of the mixture

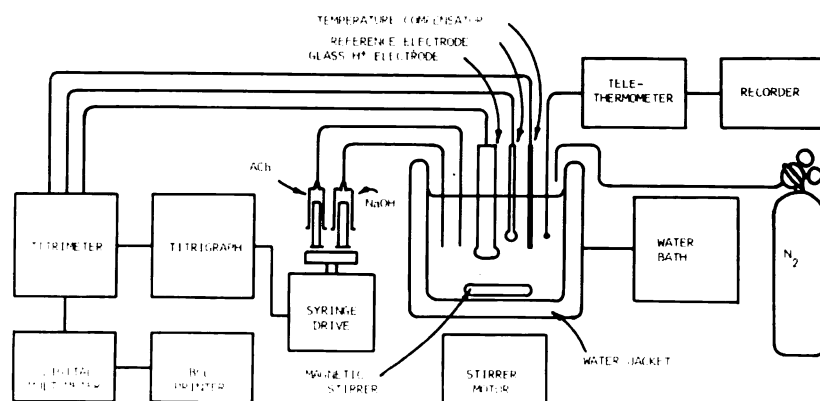


Figure 7

eliminated background activity arising from absorption of atmospheric CO_2 . A magnetic stirring bar provided rapid mixing of the reaction solution. Voltage output from the automatic titrator proportional to the pH was introduced into a Fairchild Digital Multimeter model 7000A. Output from the multimeter was introduced into an American Instrument Co. BCD printer model 4500. Sampling the voltage every 5 sec and printing voltages proportional to the pH permitted monitoring of the pH. It was determined that the pH was held within 0.02 pH units of the pre-set pH value. Reaction mixture temperature was set and maintained by a Forma Scientific waterbath model 2096 reliable to $\pm 0.1^\circ \text{C}$. The reaction mixture temperature during the reaction was monitored using a Yellow Springs Instrument tele-thermometer system with a Hitachi-Perkin-Elmer model 159 recorder providing continuous graphical output.

The reaction mixture, unless otherwise indicated, initially contained 0.01% gelatine, 1.2 mM acetylcholine chloride, which was shown to saturate the 240000 molecular weight brain and eel forms of the enzyme or 0.8 mM which was saturating for the 60000 molecular weight species. The reaction was started by the addition of 50 μl of enzyme (1.62×10^{-12} mols AChE).

Assays were performed in the absence of added inorganic salts, since salts have specific effects at the peripheral site on the enzyme (Roufogalis & Thomas, 1968) and decrease the Ca^{2+} effect. In studies examining the influence of pH and temperature on reaction rate, initial pH values were set by adding 0.01 M NaOH or HCl and the rate at the set pH was then measured. The rates were

determined at 10 to 15 pH values usually from pH 6.8 to 8.1.

After determining the reaction rate pH dependence under the above conditions, the pH dependence was re-determined after the addition of 1 ml of 1 $\underline{\text{M}}$ CaCl_2 , raising the Ca^{2+} concentration to 10 $\underline{\text{mM}}$. This Ca^{2+} concentration was found to provide the maximum acceleratory effect and was used throughout (Figure 13). After the pH dependence in the presence and absence of Ca^{2+} was determined at the initial temperature in the presence and absence of CaCl_2 , a new reaction mixture was prepared and the procedure was repeated at a different temperature. Usually five or six temperatures were examined ranging from 10° C to 35° C. The pK of the reaction was estimated from the pH vs. rate relationship using an ideal ionization curve fitted to the data points (See Appendix for Method). Volume changes, accompanying the additions of NaOH, acetylcholine, CaCl_2 , and HCl were limited to less than 5% which was accounted for within the experimental error of determinations of the rate constants (6%). In some experiments with both brain and eel enzyme 100 $\underline{\text{mM}}$ NaCl was present throughout. The use of 100 $\underline{\text{mM}}$ NaCl in the reaction mixture permitted comparisons of results with those obtained by other investigators (Wilson & Cabib, 1956; Heilbronn, 1965) who used similar NaCl concentrations.

The apparent $\underline{\text{K}_m}$ was estimated using a computer generated hyperbolic best fit program (See Appendix). For $\underline{\text{K}_m}$ estimations, the enzyme was added to the reaction mixture containing 0.01 % gelatine and then substrate added incrementally until saturation was reached. A new reaction mixture containing 10 $\underline{\text{mM}}$ CaCl_2 was

prepared and the procedure repeated. The K_m values (25° C) were obtained from measurements at substrate concentrations including at least two concentrations below K_m .

Some of the calculations were based upon the following relationships:

$$v = \frac{V S}{K_m + S} \quad (1) \quad V = k E \quad (2)$$

where v is the observed reaction velocity, V is the maximum reaction rate, S is the substrate concentration, k is the reaction rate constant, and E is the concentration of enzyme catalytic sites present.

Determination of acetylation rate constants (k_{+2}), de-acetylation rate constants (k_{+3}), and thermodynamic activation parameters

Figure 8 illustrates the Arrhenius relationship for eel acetylcholinesterase catalyzed acetylcholine hydrolysis in the presence of 100 mM NaCl. A similar relationship for brain enzyme (240000 molecular weight form) is given in Figure 9. The pronounced curvature ($\log k$) noted in the presence of NaCl has been previously reported (Wilson & Cabib, 1956) and may be expected for a two or more step catalytic mechanism. The mechanism has been described as in Fig. 1.

Providing that k was rate determining over the entire experimental temperature range, plots of $\log k$ vs. T^{-1} should yield straight lines. Generally, however, for a two step process, each with a different temperature dependence, one straight line would be seen over one temperature range in which one step were rate limiting and a second,

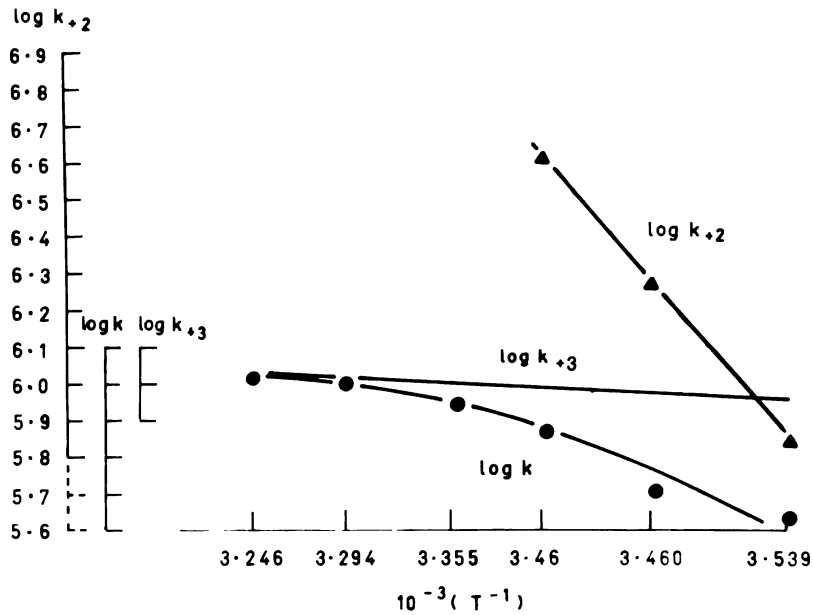


Figure 8: Representation of derived rate constants for acetylation (k_{+2}) and de-acetylation (k_{+3}) from the Arrhenius plots of eel acetylcholinesterase catalyzed acetylcholine hydrolysis in 100 mM NaCl. Enzyme activity was measured by the pH-stat method with standard assay conditions as indicated in Table XVII. Values of $\log k$ were computed from the relationship $V_{max} = kE$. k_{+3} values were derived from the asymptote of the $\log k$ versus reciprocal absolute temperature plot and k_{+2} values were computed from the relationship $1/k = 1/k_{+2} + 1/k_{+3}$.

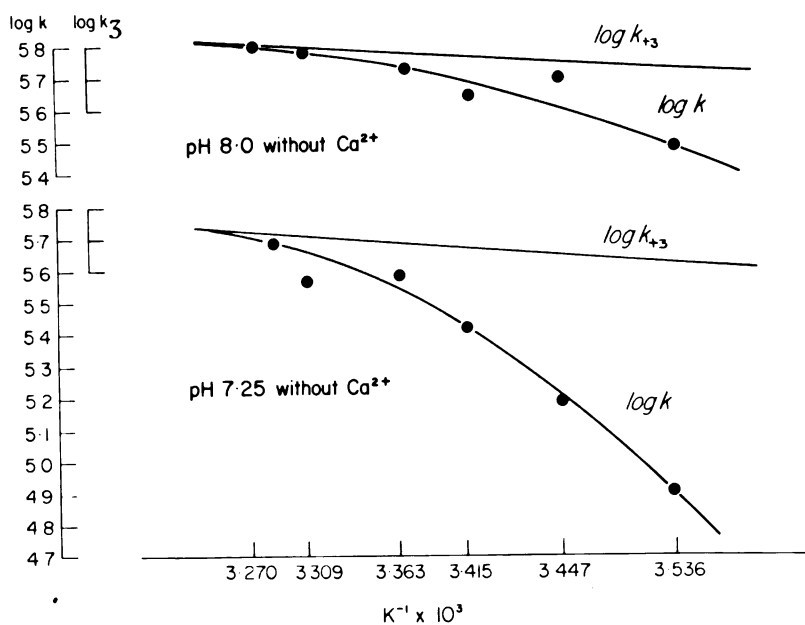


Figure 9: Representation of derived rate constants for acetylation (k_{+2}) and de-acetylation (k_{+3}) from the Arrhenius plots of brain acetylcholinesterase (mol. wt. 240000) catalyzed acetylcholine hydrolysis. Enzyme activity was measured by the pH-stat method with standard assay conditions as indicated in Table IV. Values of the rate constants were determined as indicated in Figure 8.

different straight line would be seen corresponding to the temperature range in which the second step is rate limiting. These two straight lines may be joined by a curved portion in the temperature range in which both velocity constants have similar values. It follows that, as the temperature is increased, the rate approaches that having the lower activation energy and as a consequence, the two step process should yield a curve flattening towards the higher temperatures(Wilson & Cabib,(1956). Curved Arrhenius plots similar to those reported for eel enzyme have been noted in Arrhenius plots of brain enzyme catalyzed acetylcholine hydrolysis. (Figures 8 and 9)

The preceding kinetic mechanism description, assuming steady-state conditions, yields the following relationship (Wilson & Cabib, (1956).

$$v = \frac{k_1 E S}{\left(\frac{k_{-1} + k_2}{k_1} \right) \left(1 + \frac{k_3}{k_2} \right) + S} = \frac{V S}{K_m + S} \quad (4)$$

$$\text{where } k_{-1} = k_{+2} + k_{+3}$$

As shown in Figure 8, an asymptote may be drawn to the curve. The slope of the line approximates the temperature dependence of the de-acetylation rate constant from which k_{+3} can be estimated (Wilson & Cabib, 1956). Using the measured values of k_1 and the estimated k_{+3} , k_{+2} (acetylation) may be calculated from the relationship (4). The temperature dependence was determined. The original curve was drawn by using a catenary to form a hyperbola which was fit to the data-points.

The deviation of the points from the line was measured and from these measurements a correlation coefficient and the variability of the best-fit line calculated (Appendix). In some cases, extrapolation beyond the data points was required to draw the asymptote. In these instances, variances in the values of y ($\log k$) for extrapolated x values ($1/T$) were determined in order to estimate the accuracy of the asymptote. Curved Arrhenius plots derived from brain enzyme were fit to hyperbolas in the above manner and found to have correlation coefficients of 0.970 to 0.997. Subsequently, the asymptotes were determined and values of k_{+3} and k_{+2} calculated in the manner described above. Error associated with k_{+3} values determined in this way were found to be between 10 to 20% of the mean value of the rate constant. The statistical tests used are indicated in the Appendix.

Combining equations (1), (2), and (4)

$$\underline{K_m'} = \frac{(k_{-1} + k_{+2}) k_{+1}}{(1 + (k_{+2} + k_{+3}))} \quad (5)$$

Multiplying the above relationship, equation 5, by

$(1 + (k_{+2} / k_{+3}))$ yields the following relationship:

$$\underline{K_m} = \frac{(k_{-1} + k_{+2})}{k_{+1}} \quad (6)$$

In certain experiments examining the effect of pH on the derived $\underline{K_m}$ (6), the values of k_{+2} and k_{+3} were derived as indicated earlier.

Activation enthalpies and entropies were estimated from plots of $\log k_{+2}$ or $\log k_{+3}$ vs. reciprocal absolute temperature. Calculations were based upon the following Arrhenius and transitions-state-

theory relationships (Laidler & Bunting, 1973).

$$\log k_n = \frac{-E_{act}}{2.303 R T} + \log A \quad (7)$$

$$\Delta H^\ddagger = E_{act} - R T \quad (8)$$

$$\Delta G^\ddagger = -RT \ln \frac{k h}{k_b T} \quad (9)$$

$$\Delta G^\ddagger = \Delta H^\ddagger - T \Delta S^\ddagger \quad (10)$$

As can be seen from equation (7), plots of $\log k_n$ vs. $\frac{1}{T}$ result in slopes equal to $-\frac{E_{act}}{2.303 R}$, where E_{act} is the energy of activation, R is the gas constant ($1.986 \frac{\text{cal-mol}^{-1}}{\text{deg}^{-1}}$), and A is a statistical factor. ΔH^\ddagger , the enthalpy of activation, is calculated from the relationship given in equation (8). Free energies of activation, ΔG^\ddagger can be calculated from equation (9) in which k_b is the Boltzmann constant ($1.38 \times 10^{-16} \text{ erg-deg}^{-1}$), h is Planck's constant ($6.624 \times 10^{-27} \text{ erg-sec}$), T is the absolute temperature, and S^\ddagger , the entropy of activation is derived from equation (10).

RESULTS

I.

KINETIC ANALYSIS OF CALCIUM ACTIVATION OF BRAIN ACETYLCHOLINESTERASE FORMS

A. Effect of pH on kinetic constants

As shown in Table IV, the rate constants for acetylation (k_{+2}), catalyzed by the 240000 molecular weight brain acetylcholinesterase form, were more pH dependent, both in the presence and absence of Ca^{2+} , than those for de-acetylation (k_{+3}). As the pH was increased from 7.25 to the pH optimum of 8.0, acetylation was enhanced two to four-fold in the absence and about two-fold in the presence of Ca^{2+} . In contrast, de-acetylation, either in the presence or absence of Ca^{2+} , increased by only 30 to 40% as the pH optimum was approached (Table IV). At all pH values, Ca^{2+} additions resulted in a marked acceleration (two to four-fold) of acetylation, whereas Ca^{2+} accelerated the de-acetylation process by only 30% (Table V). The ratios of acetylation/ de-acetylation show that de-acetylation is the rate determining step for acetylcholine hydrolysis catalyzed by this brain enzyme form at 20° C (Table V). In addition, the ratios indicate that the contribution of k_{+2} to the observed k (see equation (4)) varies from 33% (pH 7.25) to 12% (pH 8) in the absence of Ca^{2+} and from 17% (pH 7.25) to 10% (pH 8) in the presence of Ca^{2+} . As indicated in Table , the ratio of acetylation/de-acetylation shows that

Table IV

240000 MOLECULAR WEIGHT BRAIN ACETYLCHOLINESTERASE FORMpH dependence of the overall rate constant (k_{+2}), acetylation rate constant(k_{+1}), and de-acetylation rate constant (k_{+3})

		<u>pH</u>			
		<u>7.25</u>	<u>7.5</u>	<u>7.75</u>	<u>8.0</u>
-6	-1				
10	k (min ⁻¹) ₂₊	0.31	0.36	0.43	0.57
without Ca					
-6	-1				
10	k (min ⁻¹) ₂₊	0.56	0.57	0.64	0.76
with Ca					
-6	-1				
10	k (min ⁻¹) ₂₊	0.89	0.98	1.85	3.67
without Ca					
-6	-1				
10	k (min ⁻¹) ₂₊	3.48	3.50	6.74	7.42
with Ca					
-6	-1				
10	k (min ⁻¹) ₂₊	0.47	0.56	0.56	0.68
without Ca					
-6	-1				
10	k (min ⁻¹) ₂₊	0.67	0.68	0.76	0.84
with Ca					

The enzyme active was measured by the titrimetric method with standard assay conditions of 0.01% gelatine, 1.2 mM acetyl-

choline chloride, 1.62×10^{-12} mols acetylcholinesterase, at 20° C, in a total volume of 100 ml. The CaCl₂ concentration was 10 mM.

The data was obtained from two sets of experiments with errors associated with the experimentally determined k and the derived k values as reported in Methods.

+3

Table V

240000 MOLECULAR WEIGHT BRAIN AChE FORM

pH dependence of the ratios of reaction rate constants in the
presence and absence of Ca²⁺

	<u>pH</u>			
	7.25	7.5	7.75	8.0
$\frac{k (+ Ca)}{k (- Ca)}$	1.81	1.58	1.49	1.33
$\frac{k_{+2} (+ Ca)}{k_{+2} (- Ca)}$	3.91	3.57	3.64	2.02
$\frac{k_{+3} (+ Ca)}{k_{+3} (- Ca)}$	1.43	1.21	1.36	1.24
$\frac{k_{+2} (+ Ca)}{k_{+3} (+ Ca)}$	5.2	5.1	8.9	8.8
$\frac{k_{+2} (- Ca)}{k_{+3} (- Ca)}$	1.9	1.8	3.3	5.4

Enzyme activity was measured by the pH-stat method with standard assay conditions of 0.01% gelatine, 1.2 mM acetylcholine chloride,
-12

1.62×10^{-12} mols acetylcholinesterase at 20° C, in a total volume of 100 ml. That data was obtained from two sets of experiments with errors associated with the experimentally determined k and the derived k values as reported in Methods.

+3

de-acetylation is also the rate determining step for acetylcholine hydrolysis catalyzed by the 60000 molecular weight form and that the contribution of acetylation to the overall rate varies in a manner similar to that observed for the 240000 molecular weight species (Table V). Enhancement of acetylation by Ca^{2+} is also noted in the 60000 molecular weight form, although the degree of rate acceleration is less than that observed in the larger species. In the smaller form (Table VII), the ratio of the overall velocity constant, k , (with Ca^{2+} / without Ca^{2+}) varies with pH in a manner that parallels the pH dependence of the ratio of the rate determining de-acetylation rate constant k_{+3} (with Ca^{2+} / without Ca^{2+}). In contrast, in the reaction catalyzed by the 240000 molecular weight form, the ratio of the overall velocity constant, k , (with Ca^{2+} / without Ca^{2+}), increased markedly (33 to 81%) with decreasing pH, whereas the ratio of the rate determining de-acetylation rate constant k_{+3} , (with Ca^{2+} / without Ca^{2+}) remained relatively constant (average value of 1.31). This result suggests that, in the case of the larger enzyme form, factors in addition to the Ca^{2+} effect upon de-acetylation are required to account for the observed pH dependency of the ratio of the overall velocity constant, k , (with Ca^{2+} / without Ca^{2+}).

As shown in Figure 10, analysis of pH vs. rate profiles for acetylcholine hydrolysis catalyzed in the presence and absence of Ca^{2+} by the 240000 molecular weight brain form revealed a pK shift of approximately 0.22 ± 0.05 pH units (14 determinations). This shift was not temperature dependent and was consistently observed. Analysis of pH vs. rate profiles for reactions catalyzed by the 60000 molecular weight species revealed two pK's, one of approximately pH 6.7 ± 0.05 and

Table VI

60000 MOLECULAR WEIGHT BRAIN ACETYLCHOLINESTERASE FORMpH dependence of the overall rate constant (k_{+2}), acetylation rate constant (k_{+2}^{-6}) and de-acetylation rate constant (k_{+3}^{-1})

		<u>pH</u>			
		7.0	7.25	7.50	7.75
10^{-6}	k_{+2}^{-1} without Ca	0.47	0.52	0.51	0.61
10^{-6}	k_{+2}^{-1} with Ca	0.53	0.64	0.75	0.86
10^{-6}	k_{+2}^{-1} without Ca	1.84	2.58	4.70	4.57
10^{-6}	k_{+2}^{-1} with Ca	2.47	3.80	8.92	12.50
10^{-6}	k_{+3}^{-2+} without Ca	0.59	0.62	0.60	0.77
10^{-6}	k_{+3}^{-2+} with Ca	0.71	0.76	0.89	1.01

The enzyme activity was measured by the titrimetric method with standard assay conditions of 0.01% gelatine, 0.8mM acetylcholine chloride, 1.57×10^{-12} mols acetylcholinesterase, at 20° C,

in a total volume of 100 ml. The CaCl_2 concentration was 10 mM.

The data was obtained from two sets of experiments with errors associated with the experimentally determined k_{+2} and the derived k_{+3} values as reported in Methods.

Table VII

60000 MOLECULAR WEIGHT BRAIN AChE FORM

pH dependence of the ratios of rate constants in the presence and
absence of Ca²⁺

	<u>pH</u>			
	7.25	7.5	7.75	8.0
$\frac{k (+Ca)}{k (-Ca)}$	1.13	1.23	1.47	1.41
$\frac{k_{+2} (+Ca)}{k_{+2} (-Ca)}$	1.34	1.47	1.90	2.74
$\frac{k_{+3} (+Ca)}{k_{+3} (-Ca)}$	1.20	1.23	1.48	1.31
$\frac{k_{+2} (+Ca)}{k_{+3} (+Ca)}$	3.5	5.0	10.4	12.4
$\frac{k_{+2} (-Ca)}{k_{+3} (-Ca)}$	3.1	4.2	7.8	5.9

Enzyme activity was measured by the pH-stat method with standard assay conditions of 0.01% gelatine, 0.8 mM acetylcholine chloride,
-12

1.57×10^{-12} mols acetylcholinesterase, at 20° C, in a total volume of 100 ml. The data was obtained from two sets of experiments with errors associated with the experimentally determined k and the derived k values as reported in Methods.

+3

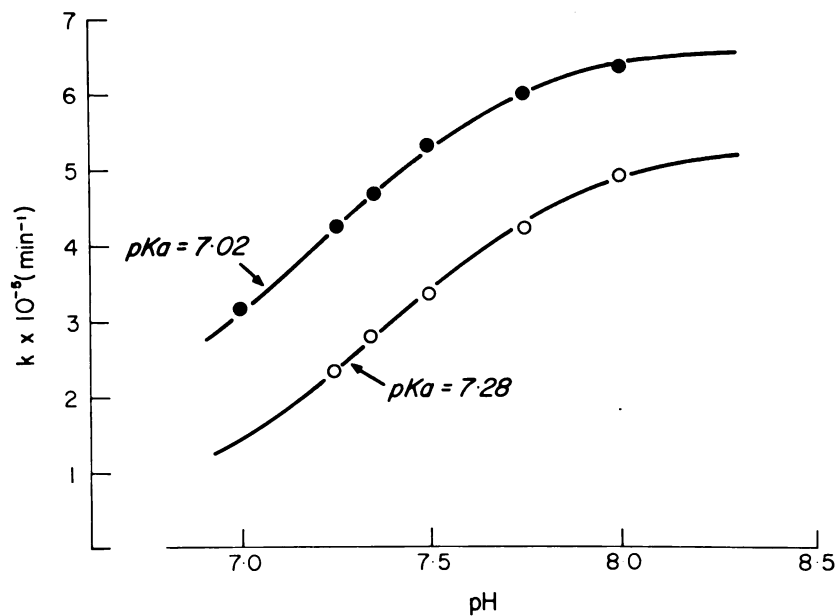


Figure 10: Reaction rate versus pH profiles of the 240000 molecular weight brain AChE catalyzed acetylcholine hydrolysis. Enzyme activity was measured by the pH-stat method with standard assay conditions as indicated in Figure 9. ○, in the absence of added ions; ● in the presence of 10 mM CaCl₂.

a second of approximately 7.45 ± 0.05 pH units (Figure 11). However, neither of these pK values were altered in the presence of Ca^{2+} (Table VIII).

B. Calcium effects on thermodynamic activation parameters

A statistical analysis of each reaction step for a particular enzyme form does not reveal a clear cut distinction in the relative contribution of ΔS^\ddagger and ΔH^\ddagger in the Ca^{2+} acceleration process (Tables IX-XII). However in the Ca^{2+} mediated case a more favorable acetylation ΔG^\ddagger values for both brain forms is due to a more favorable ΔS^\ddagger value ($P < 0.001$) (comparing $\Delta S^\ddagger \pm \text{Ca}^{2+}$) with little likelihood of a change in ΔH^\ddagger value ($P < 0.9$) (comparing $\Delta H^\ddagger \pm \text{Ca}^{2+}$). The possibility of a similar process for the de-acetylation step can be proposed only in a very tentative manner because the difference in $\Delta H^\ddagger \pm \text{Ca}^{2+}$ is significant only at $P < 0.4$ and the difference in $\Delta S^\ddagger \pm \text{Ca}^{2+}$ is significant at $P < 0.3$.

C. Calcium effects on K_m

Table XIII illustrates that, in the case of the larger enzyme form, the K_m is higher in the presence of Ca^{2+} at all pH values except 7.25. The derived K_m is equal to :

$$\left(\frac{k_{-1} + k_{+2}}{k_{+1}} \right) \quad (8)$$

and the effect of Ca^{2+} on the derived K_m can be further analyzed by examining the influence of Ca^{2+} on the acetylation rate constant (k_{+2}).

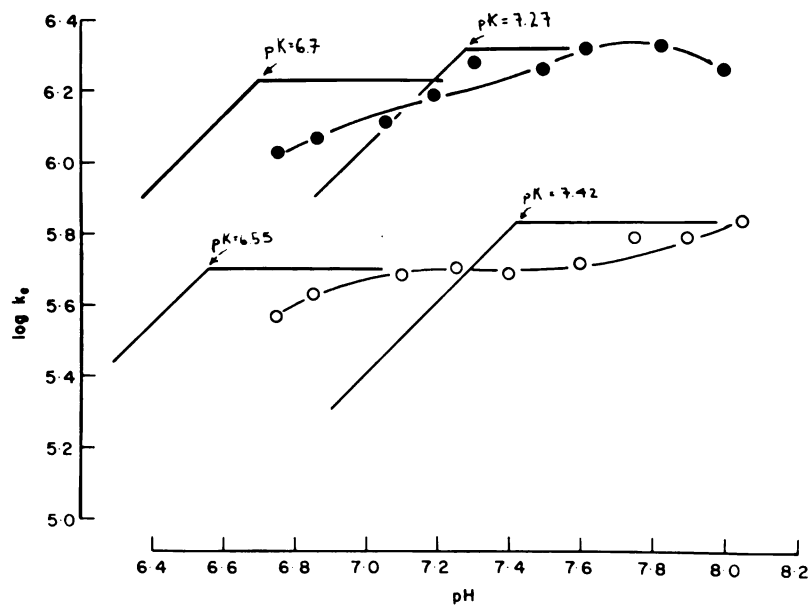


Figure 11: Estimation of pK values associated with the 60000 molecular weight brain AChE catalyzed hydrolysis of acetylcholine. The method of determination of pK values is described in the Appendix. Enzyme activity was measured using the pH-stat method with standard assay conditions as described in the legend of Table VII. (○), in the absence of CaCl₂ ; (●), in the presence of

10 mM CaCl₂ .

Table VIII

60000 MOLECULAR WEIGHT BRAIN AChE FORM

Effect of temperature and Ca^{2+} on the two reaction apparent
pK's

Temperature (° C)	pK ₁		pK ₂	
	without Ca^{2+}	with Ca^{2+}	without Ca^{2+}	with Ca^{2+}
	8.5	6.87	6.8	7.3
15	6.7	6.7	7.5	7.55
20.5	6.55	6.8	7.45	7.3
25.5	6.25	6.5	7.65	7.3
30	6.55	6.55	7.75	7.5

The apparent pK values were estimated according to the procedure outlined in the Appendix.

Table IX

240000 MOLECULAR WEIGHT BRAIN ACETYLCHOLINESTERASE FORM

Thermodynamic activation parameters for acetylation in the
presence and absence of Ca²⁺

pH	ΔG^\ddagger (kJ mol ⁻¹)		ΔH^\ddagger (kJ mol ⁻¹)		ΔS^\ddagger (J mol ⁻¹ K ⁻¹)	
	with Ca ²⁺	without Ca ²⁺	with Ca ²⁺	without Ca ²⁺	with Ca ²⁺	without Ca ²⁺
8.0	44.3	46.0	75.2	74.8	+105.5	+ 98.2
7.75	44.6	46.4	80.3	93.2	+144.0	+137.5
7.5	45.8	48.6	76.5	73.6	+ 99.8	+ 90.4
7.25	46.5	49.5	92.0	102.4	+173.0	+162.9

Thermodynamic activation parameters were calculated as indicated in Methods. Differences in the values in the presence and absence of Ca²⁺ were analyzed utilizing the paired observation test. Ca²⁺ mediated differences in ΔG^\ddagger were significant at (P < 0.01); differences in ΔH^\ddagger were significant at (P < 0.2); differences in ΔS^\ddagger were significant at (P < 0.01).

Table X

240000 MOLECULAR WEIGHT BRAIN ACETYLCHOLINESTERASE FORM

Thermodynamic activation parameters for de-acetylation in the presence
²⁺
and absence of Ca

pH	ΔG^\ddagger (kJ mol ⁻¹)		ΔH^\ddagger (kJ mol ⁻¹)		ΔS^\ddagger (J mol ⁻¹ K ⁻¹)	
	²⁺ with Ca	²⁺ without Ca	²⁺ with Ca	²⁺ without Ca	²⁺ with Ca	²⁺ without Ca
8.0	48.6	49.1	1.7	1.7	-160.2	-162.0
7.75	48.8	49.5	7.1	7.1	-142.5	-144.9
7.5	49.1	49.4	6.7	7.5	-144.9	-143.2
7.25	49.1	50.0	7.9	8.8	-140.0	-140.7

Thermodynamic activation parameters were calculated as indicated in Methods.
Differences in the values in the presence and absence of Ca²⁺ were analyzed
utilizing the paired observation test. Ca²⁺ mediated differences in ΔG^\ddagger were
significant (P < 0.01); differences in ΔH^\ddagger were significant at
(P < 0.1); Values of ΔS^\ddagger , in the presence and absence of Ca²⁺
were statistically different at (P < 0.1).

Table XI

60000 MOLECULAR WEIGHT BRAIN ACETYLCHOLINESTERASE FORM

Thermodynamic activation parameters for acetylation in the presence
²⁺
 and absence of Ca

pH	ΔG^\ddagger (kJ mol ⁻¹)		ΔH^\ddagger (kJ mol ⁻¹)		ΔS^\ddagger (J mol ⁻¹ K ⁻¹)	
	with Ca ²⁺	without Ca ²⁺	with Ca ²⁺	without Ca ²⁺	with Ca ²⁺	without Ca ²⁺
7.75	43.6	45.2	76.6	77.3	+112.7	+109.8
7.5	43.9	44.2	84.2	81.9	+137.6	+128.8
7.25	44.8	45.8	93.2	75.7	+165.3	+102.0
7.0	46.3	46.9	100.7	97.0	+186.0	+170.9

Thermodynamic activation parameters were calculated as indicated in Methods.
²⁺
 Differences in the values in the presence and absence of Ca²⁺ were analyzed
²⁺
 using the paired observation test. Ca²⁺ mediated differences in ΔG^\ddagger were
 significant (P < 0.05); differences in ΔH^\ddagger were significant at (P < 0.2);
 Values of ΔS^\ddagger were significant at (P < 0.2)

Table XII

60000 MOLECULAR WEIGHT BRAIN ACETYLCHOLINESTERASE FORM

Thermodynamic activation parameters for de-acetylation in the presence
and absence of Ca²⁺

pH	ΔG^\ddagger (kJ mol ⁻¹)		ΔH^\ddagger (kJ mol ⁻¹)		ΔS^\ddagger (kJ mol ⁻¹ K ⁻¹)	
	with Ca ²⁺	without Ca ²⁺	with Ca ²⁺	without Ca ²⁺	with Ca ²⁺	without Ca ²⁺
7.75	48.1	48.8	1.3	1.7	-159.9	-160.9
7.75	48.4	49.4	6.7	7.1	-142.5	-144.5
7.5	48.7	49.1	5.4	4.2	-147.8	-153.4
7.25	48.9	49.3	5.9	6.3	-146.9	-146.9

Thermodynamic activation parameters were calculated as indicated in Methods. Differences in the values in the presence and absence of Ca²⁺ were analyzed utilizing the paired observation test. Ca²⁺ mediated differences in ΔG^\ddagger were significant ($P < 0.02$); differences in ΔH^\ddagger were significant at ($P > .9$); Values for ΔS^\ddagger were significant at ($P < .2$)

Table XIII

240000 MOLECULAR WEIGHT BRAIN ACETYLCHOLINESTERASE FORM

Influence of pH and Ca²⁺ on the apparent K_m

pH	<u>K_m</u> (M)		$\frac{\text{K}_m \text{ with Ca}^{2+}}{\text{K}_m \text{ without Ca}^{2+}}$
	without Ca ²⁺	with Ca ²⁺	
8.0	0.7×10^{-4}	1.8×10^{-4}	2.5
7.75	1.3×10^{-4}	2.3×10^{-4}	1.7
7.5	0.5×10^{-4}	1.5×10^{-4}	3.1
7.25	1.5×10^{-4}	1.5×10^{-4}	1.0

Enzyme activity was measured by the titrimetric method with standard assay conditions of 0.01% gelatine, acetylcholine chloride concentrations from 0.04 to 3.0 mM, 1.62×10^{-12} mols acetylcholinesterase, 10 mM CaCl₂, at 25° C. Computer generated best-hyperbolic fit analysis was

used for the K_m determination with computer generated error estimate of approximately 10%. As estimated,

$$\underline{K_m} = \frac{(k_{-1} + k_{+2}) / k_{+1}}{(1 + (k_{+2} / k_{+3}))}$$

If the value of k_{+2} contributed significantly to the value of the derived K_m , then pH dependent changes in the value of the acetylation rate constant should be paralleled by pH dependent changes in the values of the derived K_m . As seen in Table XIV, in the absence of Ca^{2+} , there is a more than three-fold pH dependent (pH 8 to pH 7.25) decrease of k_{+2} , whereas the derived K_m value does not vary in a similar manner. The same pattern is exhibited in the presence of Ca^{2+} . These results suggest that the acetylation rate constant may not contribute significantly in equation (4) and therefore that the derived K_m may approximate K_s , the enzyme-substrate dissociation constant. Thus, the effects of Ca^{2+} on the derived K_m are probably due to changes in k_{-1} and/or k_{+1} . Since pH dependent changes in the values of the derived K_m are paralleled by changes in the value of k_{+2} in the case of the 60000 molecular weight brain AChE form, it appears that for this form k_{+2} contributes significantly to the derived K_m . Therefore the derived K_m is probably not equal to the K_s (Tables XV, XVI).

Table XIV

240000 MOLECULAR WEIGHT BRAIN AChE FORM

INFLUENCE OF pH and Ca²⁺ ON THE DERIVED K_m AND ON

k₊₂ (25° C)

pH	<u>K_m</u> (M)		$\frac{\text{K}_m \text{ with Ca}^{2+}}{\text{K}_m \text{ without Ca}^{2+}}$
	without Ca ²⁺	with Ca ²⁺	
8.0	4.2 x 10 ⁻⁴	1.6 x 10 ⁻³	3.9
7.75	8.7 x 10 ⁻⁴	1.5 x 10 ⁻³	1.7
7.5	1.5 x 10 ⁻⁴	1.2 x 10 ⁻³	8.0
7.25	4.7 x 10 ⁻⁴	1.1 x 10 ⁻³	2.3

pH	k ₊₂ (min ⁻¹)		$\frac{k_{+2} \text{ with Ca}^{2+}}{k_{+2} \text{ without Ca}^{2+}}$
	without Ca ²⁺	with Ca ²⁺	
8.00	3.5	8.8	2.5
7.75	3.4	7.3	2.2
7.5	1.2	4.8	4.0
7.25	1.1	4.0	3.6

To obtain the derived K_m, $(k_{-1} + k_{+2}) / k_{+1}$, the values of the

apparent K_m (Table XIII) are multiplied by $(1 + (k_{+2} / k_{+1}))$

(see equation (5) in which values of the acetylation and de-acetylation rate constants at 25° C are estimated by the procedure described in Methods.)

Table XV

60000 BRAIN ACETYLCHOLINESTERASE FORM

Influence of pH and Ca²⁺ on the apparent K_m for acetylcholine hydrolysis

pH	K_m (M)		$\frac{K_m \text{ with Ca}^{2+}}{K_m \text{ without Ca}^{2+}}$
	without Ca ²⁺	with Ca ²⁺	
8.0	2.3×10^{-5}	1.2×10^{-4}	5.2
7.75	3.1×10^{-5}	1.3×10^{-4}	4.2
7.5	2.6×10^{-5}	1.1×10^{-4}	4.2
7.25	2.0×10^{-5}	7.8×10^{-5}	3.9

enzyme activity was measured by the titrimetric method with standard assay conditions of 0.01% gelatine, acetylcholine

chloride concentrations from 0.02 to 3 mM, 1.52×10^{-12} mols acetylcholinesterase, 10 mM CaCl₂, at 25° C. Computer generated

best hyperbolic fit analysis was used for the K_m determination with computer estimated error of approximately 10%. As estimated

$$K_m = \left(\frac{(k_{-1} + k_{+2}) / k_{+1}}{1 + (k_{+2} / k_{+3})} \right)$$

Table XVI

60000 BRAIN ACETYLCHOLINESTERASE FORM

Influence of pH and Ca²⁺ on the derived K_m and on
k₂ (25° C)

pH	K_m (M)		$\frac{K_m \text{ with Ca}^{2+}}{K_m \text{ without Ca}^{2+}}$
	without Ca ²⁺	with Ca ²⁺	
7.75	2.9×10^{-4}	2.9×10^{-3}	10.2
7.5	3.9×10^{-4}	1.7×10^{-3}	4.2
7.25	1.8×10^{-4}	7.8×10^{-4}	4.3

pH	k ₂ (min ⁻¹)		$\frac{k_2 \text{ with Ca}^{2+}}{k_2 \text{ without Ca}^{2+}}$
	without Ca ²⁺	with Ca ²⁺	
7.75	6.5	21.7	3.4
7.5	9.2	13.3	1.4
7.25	5.7	8.8	1.5

To obtain the derived K_m , $((k_{-1} + k_{+2}) / k_{+1})$, the values of the apparent K_m (Table XV) are multiplied by $(1 + (k_{+2} / k_{+3}))$ (see equation (5) in which values of the acetylation and de-acetylation rate constants at 25° C are estimated by the procedure described in Methods)

Eel Acetylcholinesterase

A. Effect of pH on kinetic constants

As shown in Table XVII, the rate constants for acetylation (k_{+2}), catalyzed by eel acetylcholinesterase were more pH dependent, both in the presence and absence of Ca^{2+} , than those for de-acetylation (k_{+3}). As the pH was increased from 7.25 to the pH optimum of 8.0, acetylation was enhanced approximately 90% in the absence and 70% in the presence of Ca^{2+} . In contrast, de-acetylation, either in the presence or absence of Ca^{2+} increased by only 10-20% as the pH optimum was approached. At all pH values, Ca^{2+} addition resulted in acceleration of acetylation and de-acetylation with the more pronounced effect upon k_{+2} (Table XVIII). The ratios of acetylation/de-acetylation show that both steps contribute significantly to the observed k_{+2} in the presence or absence of Ca^{2+} (20° C) (Table XVIII). In the absence of Ca^{2+} , acetylation and de-acetylation contribute approximately equally, whereas in the presence of Ca^{2+} de-acetylation contributes approximately 60%. The pH independent Ca^{2+} acceleration effect of 60% on the overall velocity constant k would then appear to result from accelerations of both acetylation and de-acetylation.

Table XVII

250000 MOLECULAR WEIGHT EEL ACETYLCHOLINESTERASE FORMpH dependence of the overall rate constant (k), acetylation rate constant(k_{+2}), and de-acetylation rate constant (k_{+3})

		<u>pH</u>			
		<u>7.25</u>	<u>7.5</u>	<u>7.75</u>	<u>8.0</u>
10^{-6}	k (min ⁻¹) ₂₊ without Ca	0.53	0.65	0.72	0.76
10^{-6}	k (min ⁻¹) ₂₊ with Ca	0.85	1.02	1.11	1.14
10^{-6}	k (min ⁻¹) ₂₊ without Ca	0.99	1.45	1.41	1.88
10^{-6}	k (min ⁻¹) ₂₊ with Ca	2.03	2.36	3.16	3.32
10^{-6}	k (min ⁻¹) ₂₊ without Ca	1.13	1.20	1.45	1.27
10^{-6}	k (min ⁻¹) ₂₊ with Ca	1.46	1.79	1.72	1.72

The enzyme activity was measured by the titrimetric method with standard assay conditions of 0.01% gelatine, 1.2 mM acetylcholine, 6.77×10^{-13} mols acetylcholinesterase, at 20° C, in a total volume of 100 ml. The data was obtained from two sets of experiments with errors associated with the experimentally determined k and the derived k_{+3} values as reported in Methods.

Table XVIII

250000 MOLECULAR WEIGHT EEL AChE FORM

pH dependence of the ratios of reaction rate constants in the
²⁺
 presence and absence of Ca

	pH			
	7.25	7.5	7.75	8.0
$\frac{k (+Ca)}{k (-Ca)}$	1.6	1.6	1.6	1.5
$\frac{k_{+2} (+Ca)}{k_{+2} (-Ca)}$	2.0	1.6	2.2	1.8
$\frac{k_{+3} (+Ca)}{k_{+3} (-Ca)}$	1.3	1.5	1.2	1.4
$\frac{k_{+2} (+Ca)}{k_{+3} (+Ca)}$	1.4	1.3	1.8	1.5
$\frac{k_{+2} (-Ca)}{k_{+3} (-Ca)}$	0.9	1.2	1.0	1.5

Enzyme activity was measured by the pH-stat method with standard assay conditions of 0.01% gelatine, 1.2 mM acetylcholine chloride,
⁻¹³

6.77×10^{-13} mols acetylcholinesterase, at 20 ° C, in a total volume of 100 ml. The data was obtained from two sets of experiments with errors associated with the experimentally determined k and the derived k values as reported in Methods.

⁺³

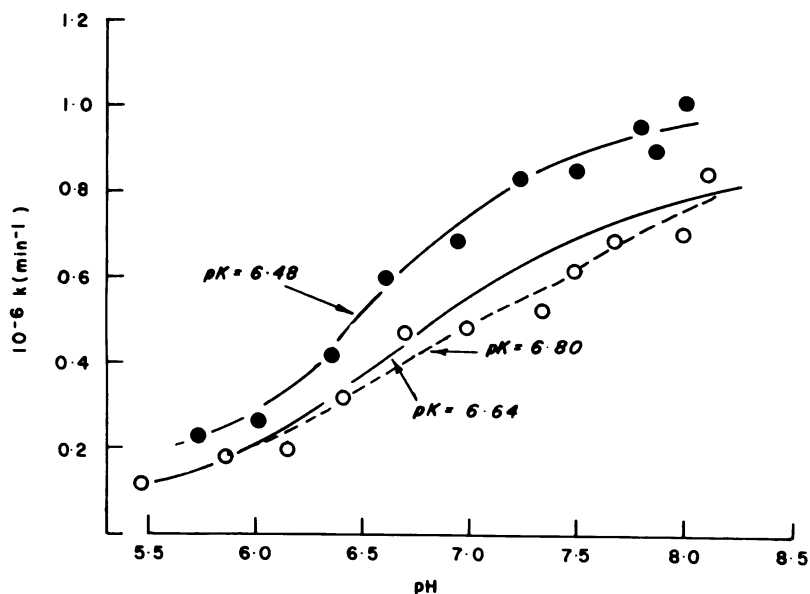


Figure 12: Analysis of pH versus rate profiles for acetylcholine hydrolysis catalyzed in the presence and absence of Ca^{2+} by eel AChE. (-----) represents the best-fit curve through the the data points. (—) represents the ideal curve determined as indicated in the Appendix. Enzyme activity was measured as described in the legend of Table XVII. The temperature was 22°C .

As shown in Figure 12 , analysis of pH vs. rate profiles for acetylcholine hydrolysis catalyzed in the presence and absence of Ca^{2+} by eel acetylcholinesterase revealed a deviation from the calculated ideal ionization curve. The deviation was apparent in the pH vs. rate profiles determined in the absence of Ca^{2+} and was observed consistently at various temperatures. Apparent pK shifts are observed if calculated from the best-fit curve drawn through the data points. However, the apparent pK shifts of as great as 0.4 pH units are reduced substantially or eliminated if calculations are based upon the ideal ionization curve.

B. Calcium effects on thermodynamic activation parameters

As suggested in Tables XIX and XX, the more favorable free energies of activation in the presence of Ca^{2+} may be due to more favorable enthalpies of activation. In addition, more unfavorable entropies of activation accompany Ca^{2+} activation, but these entropic effects are not sufficiently unfavorable to compensate for the effect on enthalpy. For acetylation, Ca^{2+} differences in ΔG^\ddagger were significant at ($P < 0.05$); differences in ΔH^\ddagger were significant at ($P < 0.1$); differences in ΔS^\ddagger were significant at ($P < 0.2$). For de-acetylation, the Ca^{2+} effects on ΔG^\ddagger were significant at ($P < 0.05$); differences in ΔH^\ddagger were significant at ($P < 0.05$); differences in ΔS^\ddagger were significant at ($P < 0.1$).

Table XIX

250000 MOLECULAR WEIGHT EEL ACETYLCHOLINESTERASE FORM

Thermodynamic activation parameters for acetylation
²⁺
 in the presence and absence of Ca

pH	ΔG^{\ddagger} (kJ mol ⁻¹)		ΔH^{\ddagger} (kJ mol ⁻¹)		ΔS^{\ddagger} (kJ mol ⁻¹ K ⁻¹)	
	with Ca ²⁺	without Ca ²⁺	with Ca ²⁺	without Ca ²⁺	with Ca ²⁺	without Ca ²⁺
8.0	44.6	45.9	74.7	89.2	+102.7	+148.2
7.75	43.6	46.6	77.1	82.5	+114.4	+122.5
7.5	45.4	46.6	74.4	86.4	+ 99.1	+136.9
7.25	46.1	47.9	65.4	65.8	+ 66.0	+ 61.4

Thermodynamic activation parameters were calculated as indicated in Methods. Differences in the values in the presence and absence of Ca²⁺ were analyzed utilizing the paired observation test. Ca²⁺ mediated differences in ΔG^{\ddagger} were significant (P < 0.05); differences in ΔH^{\ddagger} were significant at (P < 0.1); differences in ΔS^{\ddagger} were significant at (P < 0.2).

Table XX

250000 MOLECULAR WEIGHT EEL AChE FORM

Thermodynamic activation parameters for de-acetylation in the
presence and absence of Ca²⁺

pH	ΔG^\ddagger (kJ mol ⁻¹)		ΔH^\ddagger (kJ mol ⁻¹)		ΔS^\ddagger (J mol ⁻¹ K ⁻¹)	
	with Ca ²⁺	without Ca ²⁺	with Ca ²⁺	without Ca ²⁺	with Ca ²⁺	without Ca ²⁺
8.0	46.8	47.5	12.9	17.6	-115.8	-102.1
7.75	46.8	47.2	6.0	6.5	-139.3	-139.0
7.5	46.7	47.7	6.8	13.5	-136.3	-116.8
7.25	47.2	47.8	10.3	15.3	-126.0	-111.0

Thermodynamic activation parameters were calculated as indicated in Methods.

Differences in the values in the presence and absence of Ca²⁺ were analyzed

utilizing the paired observation test. Ca²⁺ mediated differences in ΔG^\ddagger were significant at (P < 0.05); differences in ΔH^\ddagger were significant at (P < 0.05); differences in ΔS^\ddagger were significant at (P < 0.1).

C. Ca^{2+} effects on K_m

The apparent K_m , $\left((k_{-1} + k_{+2}) / k_{+1} \right) / \left(1 + (k_{+2} / k_{+3}) \right)$, was

shown not to be influenced significantly by temperature (pH 7.5). The average apparent K_m in the presence of Ca^{2+} is 0.073 mM and 0.038 mM in the absence of Ca^{2+} . The computer generated error estimate of the apparent K_m was approximately 10%. The apparent K_m at 25°C in the absence of Ca^{2+} decreased slightly but significantly ($P=0.05$) with increasing pH, from approximately 0.072 mM to approximately 0.035 mM , but in the presence of Ca^{2+} , the K_m at 25°C shows no significant pH dependence ($P=0.05$) (Table XXI). The derived K_m , $\left((k_{-1} + k_{+2}) / k_{+1} \right)$, (Table XXII), at 25°C as described in Methods for the thermodynamic and kinetics section, shows no pH dependence in the presence or absence of 10 mM Ca^{2+} . The K_m both in the case of the apparent and derived values, was approximately two to three fold greater in the presence of 10 mM Ca^{2+} .

Effects of other ions on rate acceleration

The degree of rate acceleration as a function of ionic concentration of MgCl_2 , BaCl_2 , CaCl_2 , LiCl , and NaCl is shown in Figure 13. These results suggest that the degree of ionic acceleration is not solely dependent upon ionic strength, given by $I = 1/2 \sum_i m_i z_i^2$, where m is the molality, z is the ionic charge, and i represents the ionic

Table XXI

250000 MOLECULAR WEIGHT EEL AChE FORMInfluence of pH and Ca²⁺ on the apparent K_m

pH	<u>K_m</u> (M)		$\frac{\text{K}_m \text{ with Ca}^{+2}}{\text{K}_m \text{ without Ca}^{2+}}$
	with Ca ²⁺	without Ca ²⁺	
8.15	8.9 x 10 ⁻⁵	3.5 x 10 ⁻⁵	2.5
8.0	7.8 x 10 ⁻⁵	4.5 x 10 ⁻⁵	1.7
7.6	6.3 x 10 ⁻⁵	4.0 x 10 ⁻⁵	1.6
7.4	1.1 x 10 ⁻⁴	2.1 x 10 ⁻⁵	2.1
7.2	9.1 x 10 ⁻⁵	6.3 x 10 ⁻⁵	1.7
7.0	7.6 x 10 ⁻⁵	7.2 x 10 ⁻⁵	1.1

Enzyme activity was measured as described in Methods. Standard assay conditions included acetylcholine concentrations of

0.04 to 3 mM, 6.72×10^{-13} mols acetylcholinesterase, 10 mM CaCl₂,

at 25° C. Computer generated best-hyperbolic fit analysis was used for the K_m determinations with computer generated error estimate of approximately 10%. As estimated,

$$\text{K}_m = \left(\left(\frac{k_{-1} + k_{+2}}{k_{+1}} \right) / \left(1 + \left(\frac{k_{+2}}{k_{+3}} \right) \right) \right)$$

Table XXII

250000 MOLECULAR WEIGHT EEL AChE FORM

pH	K_m (M)		$\frac{K_m \text{ with Ca}^{2+}}{K_m \text{ without Ca}^{2+}}$
	without Ca ²⁺	with Ca ²⁺	
8.0	1.9×10^{-4}	3.63×10^{-4}	1.9
7.75	1.2×10^{-4}	2.89×10^{-4}	2.4
7.5	8.1×10^{-5}	4.1×10^{-4}	5.1
7.25	1.6×10^{-4}	2.8×10^{-4}	1.8

pH	k_{10} (min ⁻¹)		$\frac{k_{10} \text{ with Ca}^{2+}}{k_{10} \text{ without Ca}^{2+}}$
	without Ca ²⁺	with Ca ²⁺	
8.0	4.6	7.0	1.5
7.75	3.2	6.7	2.1
7.5	3.7	5.1	1.4
7.25	2.0	3.5	1.8

To obtain the derived K_m , $(k_{-1} + k_{+2}) / k_{+1}$, the values of the

apparent K_m (Table XXI) are multiplied by $(1 + (k_{+2} / k_{+1}))$

in which values of the acetylation and de-acetylation rate constants at 25° C are estimated by the procedure described in Methods

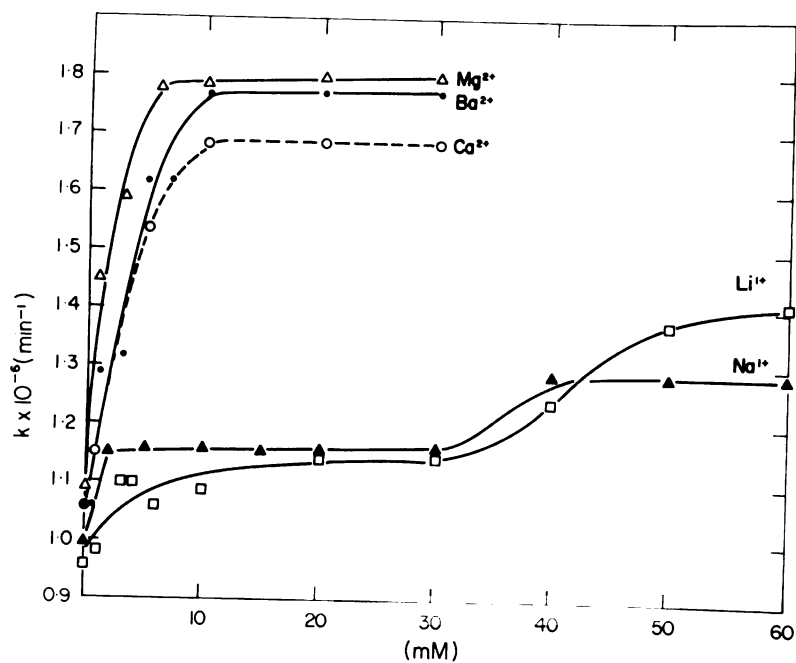


Figure 13: Ionic activation of eel AChE catalyzed acetylcholine hydrolysis. Enzyme activity was measured by the pH-stat method with standard assay conditions as described in the legend of Table XVIII. All ions as indicated were present in the form of chloride salts.

species present. For example a 10 mM solution of MgCl_2 , CaCl_2 or BaCl_2 would be equi-ionic with a 30 mM solution of NaCl or LiCl . However, in all instances the enzyme activity in the presence of the divalent cation (10 mM) is approximately 50% higher than in the presence of the monovalent cation (30 mM).

III

GRADIENT GEL ELECTROPHORESIS OF BRAIN
ACETYLCHOLINESTERASE

A. Time course experiments with forms (B) and (C) of brain acetylcholinesterase

An estimate of the molecular weight for form B of brain acetylcholinesterase was approximately 240,000 by Sephadex G-200 gel filtration but approximately 120-140000 by gradient gel electrophoresis. Initially, it was suspected that this result occurred due to dissociation as a result of the conditions of gradient gel electrophoresis. If this were to happen one would expect the transient appearance of the larger form before dissociation. To test this possibility, a time course on the gradient gel system was performed with the supposition that the 240000 molecular weight form applied might reach its equilibrium point on the gradient gel and then subsequently breakdown to the observed smaller forms. As shown in Figure 14 at 5 h and 9 h only one major component was noted. At 9 h the enzyme staining band had migrated past the region on the gel corresponding to a molecular weight of 240000. At equilibrium, 15 h., two components with molecular weights estimated at 120000 and 140000 molecular weight were found (Figure 15).

A similar experiment was performed with the smaller brain

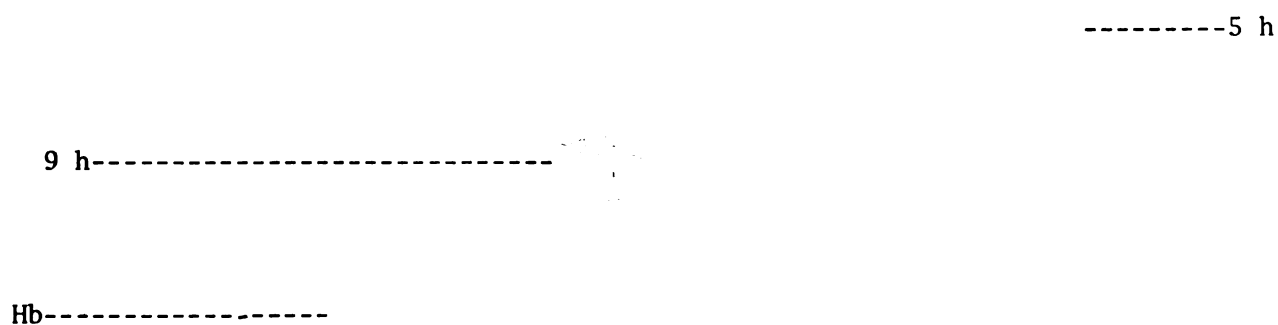


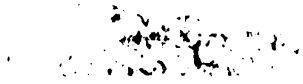
Figure 14: Gradient gel electrophoresis of brain AChE form (B) obtained from G-200. Duration of the electrophoresis was 5 h and 9 h and was pre-equilibrium. In each case approximately 0.1 μ g of enzyme was applied. Hb, hemoglobin, molecular weight 64000. General electrophoretic procedure was as described in the Methods.

-----d

-----d

-----d

Figure 14: Gradient gel electrophoresis of brain ABE form (B) obtained from 0-120. Duration of the electrophoresis was 2 h and 9 h and was pre-equilibrium. In each case approximately 0.1 g of enzyme was applied. The hemoglobin, molecular weight 66,000. General electrophoretic procedure was as described in the Methods.



15h---
140000 mol. wt.-----
----- 120000 mol. wt.
-----Hb

Figure 15: Gradient gel electrophoresis of brain AChE form (B) obtained from G-200 chromatography. Duration of the equilibrium electrophoresis run was 15 h as described in Methods. Approximately 0.1 μ g of enzyme was applied. Hb, hemoglobin, molecular weight 64000.

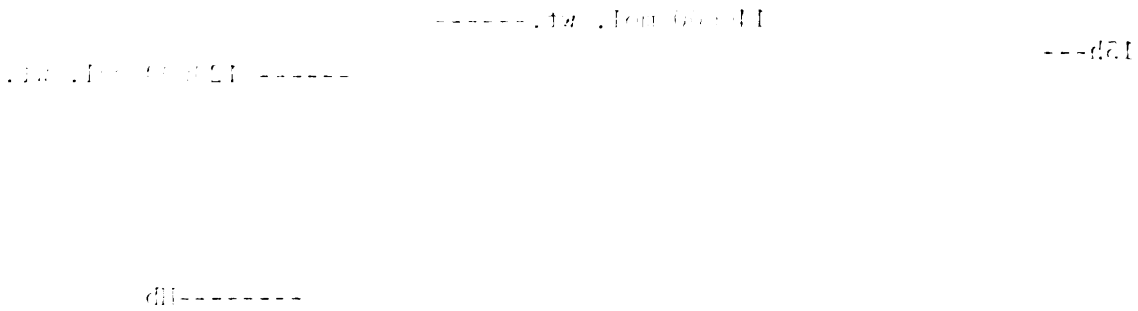


Figure 17: Gradient gel electrophoresis of brain Aβ(1-42) obtained from 6-120 chromatography. Location of the equilibrium electrophoresis run was 12 h as described in text. Approximately 0.1 μg of enzyme was applied. 15, benzylidene, molecular weight 64000.



acetylcholinesterase form. On G-200 chromatography, the the form was characterized by a molecular weight of 75000, whereas on gradient gel electrophoresis the form behaved as a 60000 molecular weight entity. It is not currently possible to determine, due to intrinsic limitations in column chromatographic and gel electrophoresis methods if the 75000 and the 60000 AChE forms are identical in terms of molecular weight . Over the same time course of electrophoresis as indicated, for the larger form, only one enzyme staining component was resolved (Figures 16 and 17).

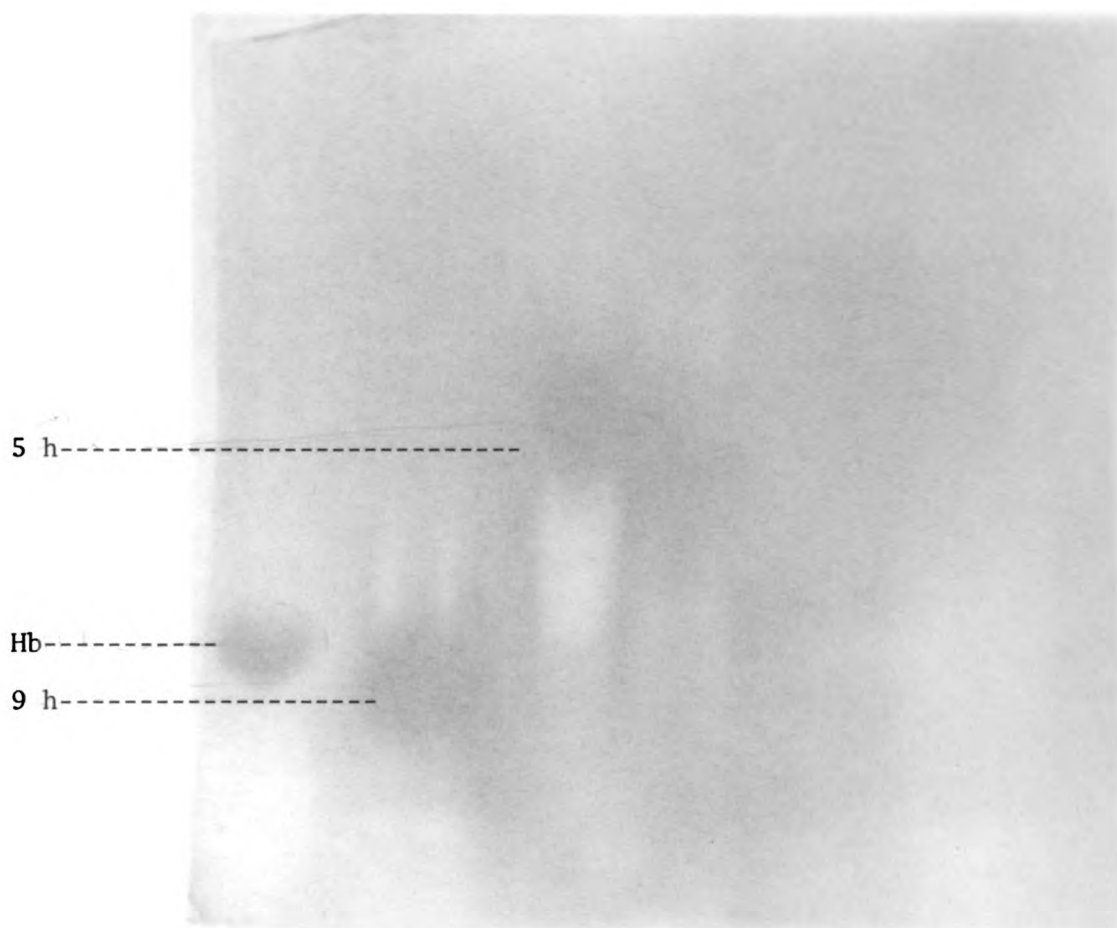


Figure 16: Gradient gel electrophoresis of brain AChE form (C) obtained from G-200 chromatography. Duration of the pre-equilibrium electrophoresis run was 5 h and 9 h. In each case approximately 0.1 μ g of enzyme was applied. General electrophoretic procedure was as described in the Methods. Hb, hemoglobin, molecular weight 64000.



Figure 16: Gradient gel electrophoresis of brain Aβ42 form (C) obtained from G-200 chromatography. Duration of the pre-equilibrium electrophoresis run was 2 h and 9 h. In each case approximately 0.1 μg of enzyme was applied. General electrophoretic procedure was as described in the Methods. IIP, homo-globin, molecular weight 64000.



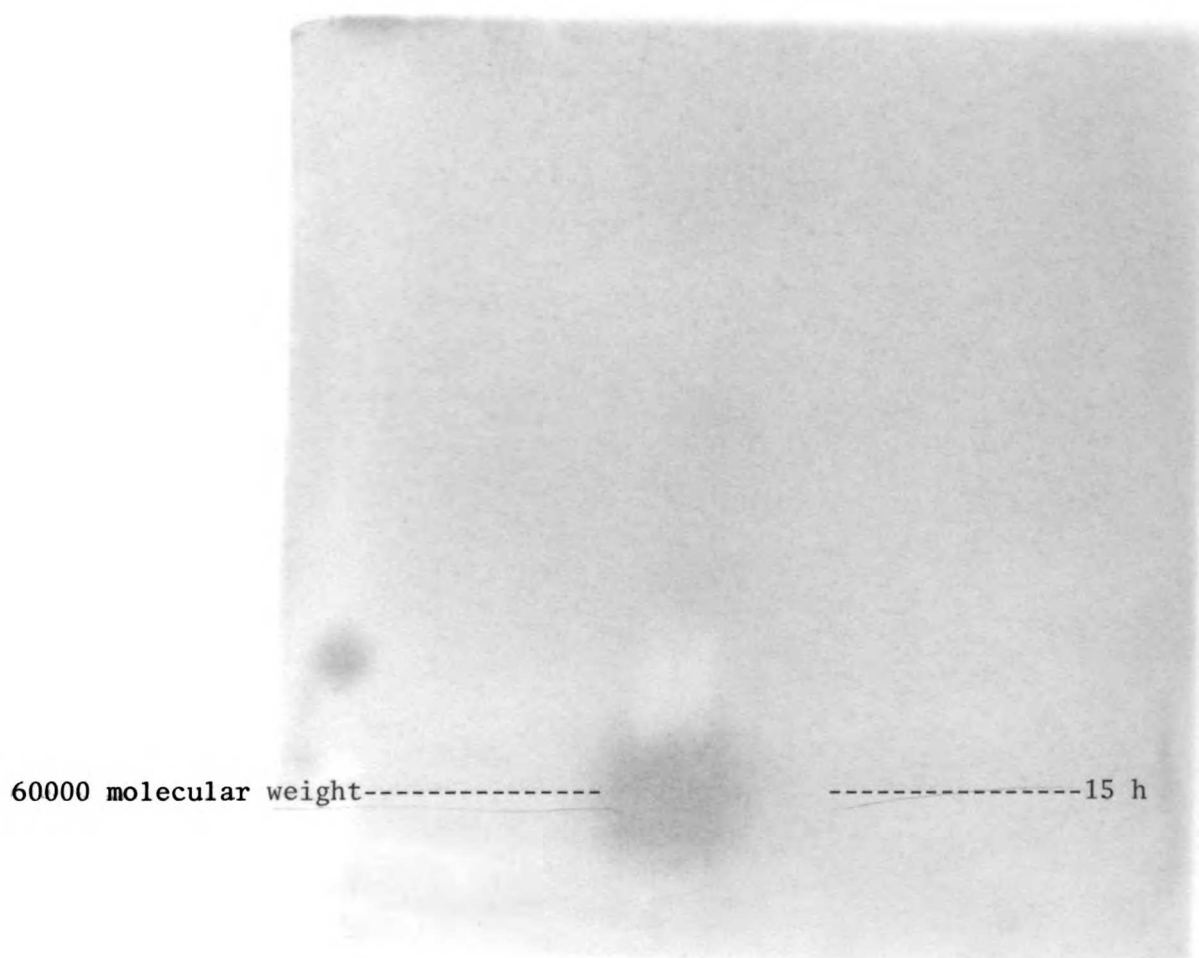
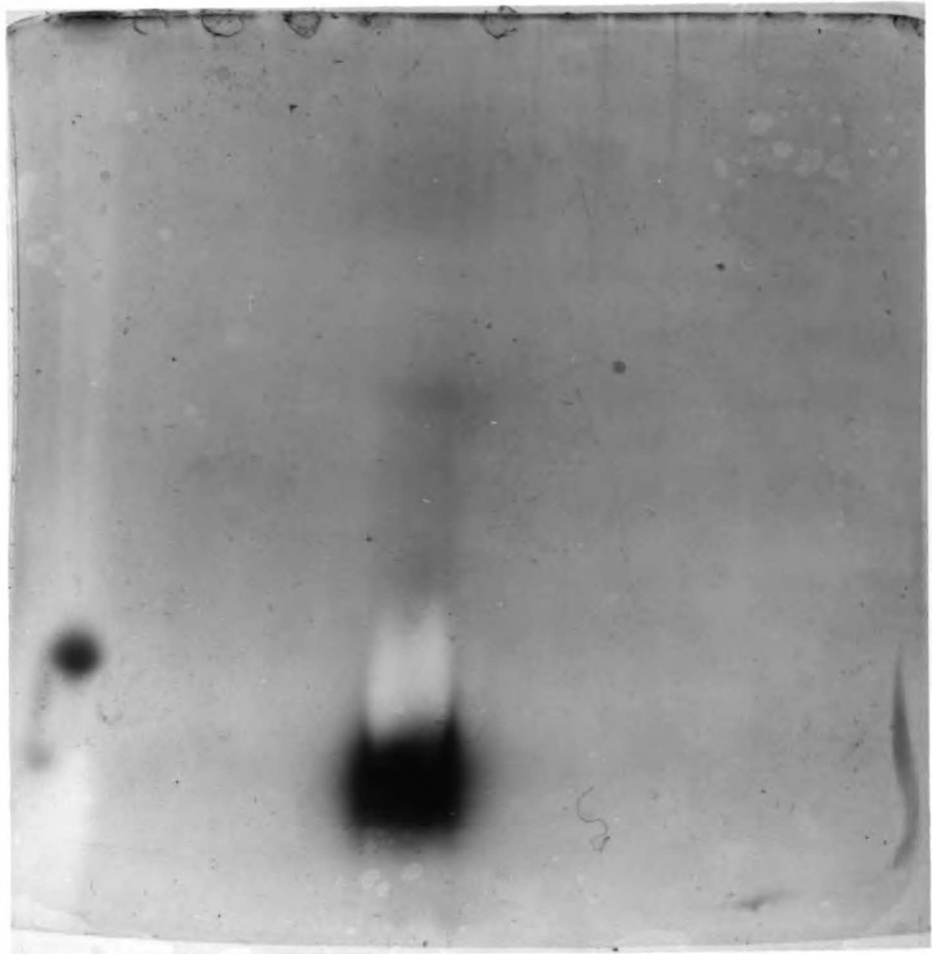


Figure 17: Gradient gel electrophoresis of brain AChE form (C) obtained from G-200 chromatography. Duration of the equilibrium electrophoresis run was 15 h as described in Methods. Approximately $0.1\mu\text{g}$ of enzyme was applied.

-----molecular weight-----
-----15 h-----

Figure 17: Gradient gel electrophoresis of brain ABE form (C) obtained from G-100 chromatography. Purification of the equilibrium electrophoresis run was 15 h as described in Methods. Approximately 0.1 g of enzyme was applied.



DISCUSSION

I.

Thermodynamic and Kinetic Analysis of Ca²⁺ Activation of Brain and Eel Acetylcholinesterase

A. pH dependence of Ca²⁺ influences on acetylcholine hydrolysis by brain and eel acetylcholinesterase

The bell-shaped pH-activity profile for acetylcholinesterase has been interpreted as representing two essential ionizable groups at the active site (Wilson & Bergman, 1950). One titratable group with a pK of about 6.7 has been suggested to be an imidazole group, associated with an essential active site histidine (Wilson and Bergman, 1950; Spencer and Sturetevant, 1959). The involvement of the serine hydroxyl moiety has been suggested by the recovery of serine phosphate from hydrolysates of di-isopropylfluorophosphate inhibited enzyme (Shaffer et al., 1953) .

In the present study de-acetylation was found to be the rate determining step in acetylcholine hydrolysis catalyzed either by the 60000 molecular weight or by the 240000 molecular weight brain enzyme form. This finding was in accord with that proposed for eel acetylcholinesterase catalyzed acetylcholine hydrolysis (Wilson and Cabib, 1956). In the case of both brain enzyme forms, Ca²⁺

enhances the rate determining de-acetylation step by about 30% over the pH range 7.25-8.0. With the 60000 molecular weight form the acceleration effect on de-acetylation (k_{+3}) parallels the Ca^{2+} effect on the ratio of the overall rate constant, k (with Ca^{2+} / without Ca^{2+}) and occurs without an effect on the pK. By contrast, the ratio of the overall rate constant, k (with Ca^{2+} / without Ca^{2+}) for the 240000 molecular weight brain enzyme form increases from 1.33 to 1.81 as the pH decreases from 8.0 to 7.25 despite a constant 30% acceleration of de-acetylation over the same pH range. A pK shift of approximately 0.2 unit is noted for the 240000 molecular weight form. It is suggested that a combination of the 30% enhancement of k_{+3} as well as the pK shift appears to account for the pH dependent degree of Ca^{2+} acceleration in the 240000 molecular weight form. As shown in Figure 18, a control curve (a) represents the pH vs. rate profile in the absence of Ca^{2+} (ideal ionization curve fit to data points). Curve b is the ideal curve from (a) shifted 0.2 pH units lower, representing the 0.2 pK shift observed with Ca^{2+} in the larger brain form. Finally, this curve is multiplied by a factor of 1.3, accounting for the Ca^{2+} mediated 30% increase in de-acetylation (curve c). The observed experimental points in the presence of Ca^{2+} (solid circles) show a coincidence with the theoretical curve which argues in favor of a Ca^{2+} effect on both pK and de-acetylation as a possible mechanism for the pH dependent degree of Ca^{2+} acceleration in the 240000 molecular weight form. Since the Ca^{2+} effects on acetylation are similar in both the 60000 and 240000 molecular weight forms, the major distinguishing feature in terms of Ca^{2+} acceleration appears to be the apparent pK shift in the larger molecular weight species.

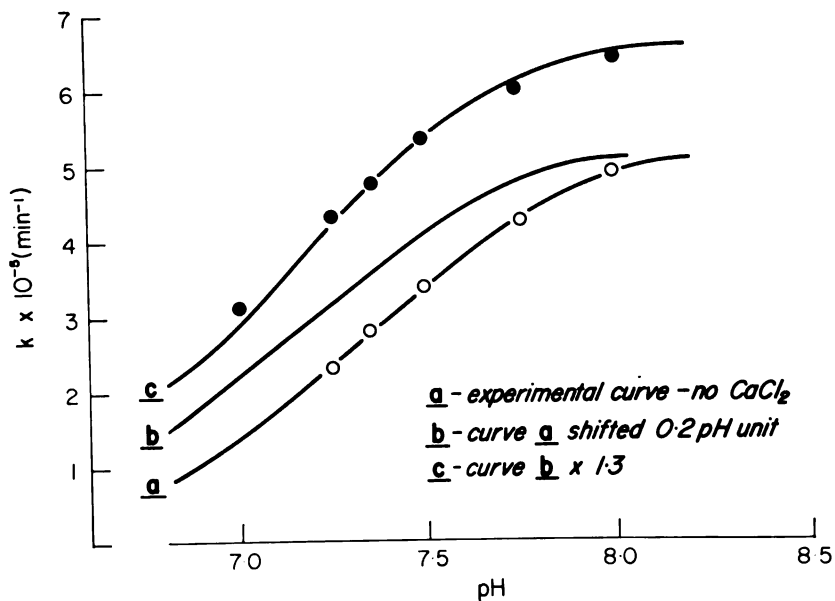


Figure 18: Reaction rate versus pH profiles of the 240000 mol. wt. brain acetylcholinesterase catalyzed acetylcholine hydrolysis. Enzyme activity was measured by the pH-stat method with standard assay conditions as described in the legend to Table IV. ○, in the absence of added ions; ● in the presence of 10 mM CaCl_2 . The control curve (a) represents the pH versus rate profile in the absence of Ca^{2+} (ideal ionization curve fit to data points). Curve b is the ideal curve from (a) shifted 0.2 pH units, representing the 0.2 pH unit pK shift observed with Ca^{2+} . This theoretical curve is shifted upwards by a factor of 1.3 (curve c), accounting for the Ca^{2+} mediated 30% increase in de-acetylation. The observed experimental points in the presence of Ca^{2+} (solid circles) show a coincidence with the theoretical curve.

It has been pointed out by Tanford (1961) that divalent cations can shift the pK of imidazole to lower values. This effect probably occurs by competition between the divalent ions and hydrogen ions for the titratable nitrogen of imidazole. Should this effect occur at the active center of acetylcholinesterase, a loss of activity should be observed, since the de-protonated form of the imidazole of histidine is thought to be required for enzyme activity. Thus it appears unlikely that Ca^{2+} association with imidazole could be responsible for the Ca^{2+} acceleratory effect.

For eel acetylcholinesterase analysis of the pH dependence of the acetylation (k_{+2}) and de-acetylation (k_{+3}) rate constants suggested that in the presence or absence of $10 \text{ mM } \text{CaCl}_2$, neither acetylation nor de-acetylation is the rate determining step. Instead, both rate constants significantly contribute to the overall velocity constant, k . This result contrasts with that obtained in $100 \text{ mM } \text{NaCl}$ in which case de-acetylation was shown to be rate determining (Figure 8). The contribution of both reaction steps to the overall rate and the greater pH sensitivity of the acetylation reaction compared to the de-acetylation reaction may provide a basis for the observed deviation from an ideal titration curve of the pH vs. rate profile as well as the apparent reaction pK shift. The deviation from ideal behavior may be responsible for at least a part of the apparent pK shift. However,

since pK shifts of approximately 0.2 pH units can occur even if calculations are based upon idealized titration curves, other factors such as those suggested below, may be involved. Deviations from ideal titration behavior were initially considered to be a possible result of experimental variability. However, repeated observation of the deviation suggested the above interpretation.

Although employing the pH dependence curve of enzyme activity to estimate ionization constants of groups involved in the catalytic process is common, it must be recognized that the estimated values are derived from the overall velocity constant. This condition for estimation is quite removed from direct measurement of the group in question by conventional titration approaches, for example in acid-base titration. As has been pointed out by Bruice and Schmir (1959), the rate constant of any equilibrium step prior to the rate determining step will become part of the kinetically determined pK value. This conclusion follows since the steady-state concentration of intermediates determine, in part, the rate of individual steps in the overall reaction scheme and as a consequence may influence, although in some cases only slightly, the rate of the rate determining step. As a result, the change in the apparent pK (0.2 units for the brain or eel enzyme) with Ca^{2+} may not represent a change in the ionization constant of imidazole, but could reflect an alteration in the values of other kinetic constants of reactions preceding the rate determining catalytic step (Figure 1). In addition, variation in the pK values may also arise from pH dependent changes in which one step among several is rate determining for the reaction (Jencks (1969); Fersht and Requena (1971)). These effects have been

discussed in detail by Fromm (1975). Although a change in the rate determining step from one step to another does not occur under the present conditions for catalysis by the brain enzyme forms, changes in the relative degree of contribution of reaction steps to the overall reaction rate may be important in the observed pK effects for catalysis by the eel enzyme. In the case of chymotrypsin there are numerous examples of alterations in pK with different substrates. For example, with acetyl-tryptophan anilides, substituent dependent downward pK shifts were observed and this result^{was} interpreted in terms of a mechanisms involving an equilibrium formation of a tetrahedral addition compound to which the histidine conjugate base at the active site forms a strong hydrogen bond (Caplow, 1969). Recent studies by Rosenberry (1975) also indicate variations in the apparent pK from 5.5 to 6.3 among several acetic acid esters hydrolyzed by eel acetylcholinesterase. In the present studies, however, the pK effects appeared to be mediated by Ca²⁺, as no substrate changes were involved.

It has been suggested that histidine and serine may be the essential amino acids at the active center in terms of catalytic function. It should be emphasized that there are limitations with regard to the use of pH activity profiles to identify essential ionizing groups. The basis of the problem relates to two major factors; the environment of the functional group and the effect of hydrogen bonding. As suggested by Fromm (1975) and others there are regions in most protein molecules that may be considered relatively hydrophobic and other regions relatively hydrophilic. In

a hydrophobic region, neutral groups such as the unionized carboxyl function will tend not to dissociate as readily as they might in a hydrophilic environment because of the lower dielectric constant. This effect is based on a difference in activity of water in the hydrophobic region. Hydrogen bonding of the potentially free proton of an acidic group, such as a carboxyl, would tend to raise the pK of the acid. In a similar way, there may be a decrease in the acidic pK of a basic group, if its free electron pair is involved in hydrogen bonding. These effects are those referred to in Caplow's (1969) interpretation of pK effects due to different interactions at the catalytic site of different substrates. The above cases are just two examples of circumstances which could modify the pK in a way as to make the use of the observed pK difficult in assigning a particular amino residue as essential in the catalytic process.

There are many examples of what might be called anomalous pK values of amino acid functions in proteins (Breslow and Gurd (1962); Murdock et al., (1966)). One of the best examples of such an effect concerns the pK of the amino group of lysine at the active center of acetoacetate decarboxylase (Schmidt and Westheimer (1971)). Jencks (1969) suggested that the first step in the decarboxylation reaction is the formation of a Schiff base between an unprotonated amino lysyl residue on the enzyme and the keto function of the substrate. Plots of the pH vs. velocity indicated that a functional group in the enzyme with a pK in the range of 5 to 7 is involved in the decarboxylation reaction. Schmidt and Westheimer (1971) used 2,4 dinitro phenyl propionate to acylate the amino groups of the decarboxylase and found that the rate of propionylation was very similar to the rate of enzyme

inactivation, and that the pH-rate profile was characterized by a monovalent type titration curve with a pK of 5.9. In addition, the acylation reaction did not occur with enzyme inhibited by compounds that react with a lysyl residue at the active site on the decarboxylase. Schmidt and Westheimer indicated that, as a result, the amino group of lysine at the active site is more acidic, by 4 pK units, than the usual amino lysine residue found in proteins.

In addition, to changes in the rate limiting step with pH change, there is also the possibility of changes in the enzyme mechanism with pH. One assumption made in studies of pH kinetics is that the mechanism governing the substrate conversion to product does not change with pH. There are, however, some examples in which this assumption may not hold. The best known example is the difference in mechanisms of acid and base catalyzed hydrolysis of esters in organic chemical reactions (Jencks, 1969). Schimerlik and Cleland (1973) have suggested in the creatine kinase enzyme system that the catalytic mechanism can change with pH alteration. Another possible complexity occurs if the ionization state of the substrate is pH dependent in the pH range over which the reaction is being studied.

As a consequence of the above considerations, it is not only difficult to identify a particular group at the active site from the reaction pK, it is also clear that a pK shift may occur by many mechanisms. In summary, pK shifts may arise from changes in contributions of each step in a reaction series to the overall rate, from changes in substrate, from changes in the hydrophobicity or hydrophilicity of the region of the protein where ionization may occur, or from changes

in hydrogen bonding. There are, however, other limitations in the study of pH on kinetic behavior.

Another general point of importance in considering pH studies of enzymes are the major kinetic assumptions and simplifications made in dealing with rate data and the basis for these considerations. The equations for the interactions between species represented in Figure 1 assume either rapid equilibrium conditions or steady-state conditions for the reactions of the substrate in which all form of the enzyme are assumed to bind the substrate with equal affinity. If these assumptions were not made, the velocity equations become exceedingly complex. The assumptions may not hold for all enzymes. For some enzymes, the reaction involving the addition and dissociation of substrate or product and the interconversion of "E"S and "E"P may be as rapid as the proton transfer reactions involved in ionizations. A complete steady-state treatment of a uni-reactant, diprotic system would yield an equation for $v/(E)$ containing 15 numerator terms, some with the substrate concentration to the second and third powers and H^+ ion concentrations to the second, third and fourth powers. The denominator would contain 117 such terms (Ottolenghi, 1971). For an reaction scheme similar to Figure 1 but including an enzyme de-protonation reaction, $EH \longrightarrow E + H^+$, there would be a required analysis of 384 different reaction patterns of types described by King and Altman (1956). However, as pointed out by Cornish-Bowden (1976) analytical convenience is not in itself a sufficient justification for assuming ionization steps to be fast and as a result utilizing the simplified reaction rate treatments. Utilizing both theoretical and experimental determinations, Cornish-Bowden (1976) has estimated the minimal

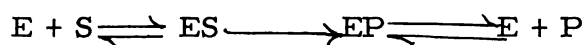
relaxation time for ionization involving the protonation of imidazole of histidine. He concludes that to the extent imidazole can be taken as a model for an ionizing group in an enzyme, it is reasonable to treat ionization steps in most enzymic reactions as equilibria. The major restriction is that the ionization should not be accompanied by a slow, compulsory change in conformation of the type noted for chymotrypsin. Thus, it would appear that the simplification of reaction rate equations in the manner described above for acetylcholinesterase reactions is reasonably based.

B. Thermodynamic activation parameters and K_m

As indicated in Results, in the case of both brain acetylcholinesterase forms both acetylation and the rate-determining de-acetylation steps are enhanced by Ca^{2+} . Thermodynamic analysis suggests that acceleration of acetylation is entropically driven. In the case of the rate-limiting de-acetylation step, the unfavorable entropy of activation, suggesting a very loose structure for the acetyl enzyme relative to the high degree of ordering of the protein and the reactant water molecule (Wilson and Cabib 1956) may be somewhat less unfavorable in the presence of Ca^{2+} . More favorable enthalpy of activations appears to be responsible for the enhanced reaction rates in the presence of Ca^{2+} for eel acetylcholinesterase catalyzed acetylcholine hydrolysis. Before discussing possible interpretations of these values in terms of enzyme mechanisms or changes in mechanisms with Ca^{2+} , a more general discussion of activation parameters is useful. A general example for an

energy versus reaction co-ordinate scheme (Segel, 1975) is presented.

Figure 19 gives an energy profile for the reaction:



Δ_1 , $E + S \rightleftharpoons E + P$, represents the overall energy difference between the unactivated product and unactivated substrate. This energy difference is characteristic for the overall process, does not depend upon the reaction pathway, and is constant regardless of whether the reaction is catalyzed by an enzyme, other organic catalysts, inorganic catalysts, or uncatalyzed. The overall reaction is characterized by an equilibrium constant, a free energy change, as well as an enthalpy and entropy change. For acetylcholine hydrolysis to choline and acetic acid, the free energy change has been found to be approximately $-12.54 \text{ kJ-mol}^{-1}$.

Δ_2 , $E + S \xrightleftharpoons[\text{K}]{\text{eq}} ES$, represents the difference in energy levels

between the ES complex and free E + free S. If energies associated with the complex and E and S are each expressed in terms of chemical potentials, then the difference in the chemical potential of the complex relative to the sum of the chemical potentials of the reactants is equal to the thermodynamic affinity. In rapid equilibrium systems,

$K_s = K_m$ and the equilibrium constant (dissociation constant)

$K_{eq} = 1 / K_s$. K_s , the dissociation constant, is usually

in the range of 10^{-6} to 10^{-2} M with a corresponding ΔG°

of -11.29 to $-11.71 \text{ kJ-mol}^{-1}$. Experimental values of K_m which are considered to represent K_s reflect values of ΔG° , free energy

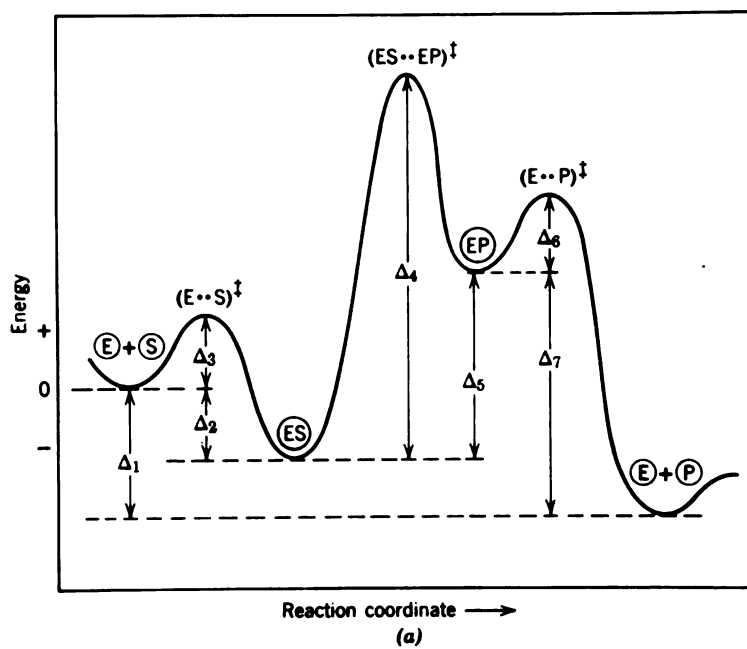


Figure 19

available to do work or what is "left over" in the process of the reaction $E + S \xrightleftharpoons{K_m} ES$. It will be of interest in the discussion of K_m values to distinguish between what Jencks has called the intrinsic binding energy and the measurable binding energy.

Δ_3 , $E + S \xrightarrow{k_1} (E \cdots S)^\ddagger$, represents the energy required to form the activated (E S) complex. The thermodynamic values associated with this step are determined by measuring the influence of temperature on k_1 . The rate of ES formation is very rapid with k_1 of the range from about 10^6 to 10^9 M⁻¹sec⁻¹.

Δ_4 , $ES \xrightarrow{k_{cat}} (ES \cdots EP)^\ddagger$, represents the bond breaking and bond making step. It has been suggested that high catalytic efficiency

(number of moles substrate converted to product per unit time per active site) is due to activation entropy effects (See Review, Jencks, 1975)

The entropy of activation may be regarded as a measure of the probability that a molecule or a pair of molecules with a certain energy can react.

With an entropy of activation greater than 0 many such molecules will react. However, with an unfavorable entropy, less than 0, probability of reaction is small. In reference to Figure 19, the value of the entropy of activation may be thought of as the width of the saddle point, Jencks (1969). A very negative ΔS^\ddagger corresponds to a narrow pass across the saddle point, so that the number of acceptable transition state configurations is small. An example of this case would be the de-acetylation reaction of the acetylated acetylcholinesterase. Jencks (1975) has regarded the role of the enzyme as a selector of proper configuration of reactants

by binding them at the active site. Particularly for the case in which the ΔS^\ddagger is very unfavorable, a large rate acceleration might be expected if the enzyme selects the few proper configurations suitable for the reaction. The enthalpies of activation may be thought of as differences in the chemical potential of the transition state structures relative to the ES complex. Accelerations in reaction rate in enzyme catalyzed reactions relative to non-enzyme catalyzed reactions usually reflect the selection of a mechanism which permits attainment of the transition state without an input of energy that is large relative to the thermal energy, $k_b T$, of the system (Mitchell, 1971).

Δ_5 , $ES \xrightleftharpoons[K_{eq}]{} EP$, represents energy differences between the two complexes ES and EP.

Δ_6 , $EP \longrightarrow (E \cdots P)^\ddagger$, represents the energy required to raise EP to a transition state for dissociation. Thermodynamic activation parameter values for this step are determined by measuring the effect of temperature on first order rate constants for dissociation of EP.

Δ_7 , $EP \xrightleftharpoons[K_{eq}]{} E + P$, represents the energy difference

between EP and free E + free P.

At this point it should be recalled that in the presence of Ca^{2+} values for the derived K_m in the case of the 240000 molecular weight form of brain acetylcholinesterase may equal K_s , the dissociation constant for enzyme and substrate.

Although the present data does not allow a similar conclusion for the case of the eel, that K_m approximates K_s has been suggested by Wilson and Cabib (1956). Thus Ca^{2+} accelerates the overall reaction, but results in a lower apparent affinity of enzyme and substrate. The relationship between these observations may follow from an interpretation of apparent K_s values and associated reaction rates made by Page and Jencks, 1971, and Jencks and Page, 1972. These investigators presented calculations indicating that there is a large entropic contribution towards the high rate constants of enzyme reactions. Multimolecular reactions in solution are thought to be slow because the bringing together of catalyst and reagent molecules involves a considerable loss of translational and overall rotational entropies (Fersht, 1974). Also, each additional molecule in the transition state of the reaction slows down the reaction by an estimated factor of up to 10^8 owing to its losing its independent translational and overall rotational entropies. Enzymatic reactions involve few independent molecules in their transition states. The independent entropy of the substrate is lost on forming the initial enzyme substrate complex and so the chemical steps involve little extra entropy loss. The effective gain in entropy is "paid for" from the binding energy of the enzyme and substrate (Fersht, 1974). In principle, then, the compensation for loss of entropy or increased restriction of movement of the reactant accompanying binding and the catalytic process is possible by using energy made available as the enzyme and substrate associate. The degree and effectiveness of this utilization may be manifest in

the apparent binding energy, determined from K_s analysis, and in the velocity of the reaction. The relation between K_s and V_{max} is clearly shown by comparing the K_m values and V_{max} values for a series of peptides hydrolyzed by pepsin. For peptides, the K_m values, determined to approximate K_s , varied over 4-fold whereas the V_{max} values varied over 1000 fold (Jencks, 1969). The conclusion was that for the substrates hydrolyzed faster, there was more effective utilization of intrinsic binding energy to promote the attainment of the transition state. If such utilization occurs, then the measured binding energy might be quite different from the true binding energy, or intrinsic binding energy, some of which may be dissipated in the unfavorable entropy compensation process discussed earlier.

There have been some attempts to estimate the intrinsic binding energy and compare the value with that obtained from measurement of the apparent binding constant. In an example given by Jencks and Page (1972), a urea molecule binding weakly to peptides and macromolecules, shows a dissociation constant when binding to avidin of 0.036 M ($\Delta G = 8.36 \text{ kJ-mol}^{-1}$). However, the addition of the intact ureido group to biotin analogs lacking this group brings about a large increase in binding energy ($K_d = 10^{-7} \text{ M}$ for the analogs and 10^{-15} M for biotin; $\Delta G = -37.62 \text{ kJ-mol}^{-1}$ and $-80.36 \text{ kJ-mol}^{-1}$ respectively). This result was interpreted to indicate that if the rotational and translational entropy requirement is satisfied by the binding of one molecule, the biotin analog to avidin, a very large increment of free energy is made available from the the additional binding of the urea group. Further, this additional energy provides

an indication of the magnitude of the intrinsic binding energy for the urea group. Other examples have been compiled recently by Jencks (1975).

The data for the acceleratory effect of Ca^{2+} on the larger brain enzyme form would generally fit this suggestion, since the higher K_s value and higher reaction rate might reflect more effective use of binding energy to facilitate the attainment of the transition state, with the energy utilized in this fashion instead of representing tight binding.

The active-site consequences of Ca^{2+} interactions with the enzyme are difficult to specify. For example, the observation of more favorable enthalpies of activation in the presence of Ca^{2+} for eel acetylcholinesterase catalyzed acetylcholine hydrolysis might result, in the case of acetylation, from an increased reactivity of the active site serine promoting easier attainment of the transition structure, occurring in this case with an apparent tightening of the structure of the transition state relative to the enzyme-substrate complex (less favorable ΔS^\ddagger in the presence of Ca^{2+}). In an analogous manner, more favorable ΔH^\ddagger for de-acetylation of the acetyl-enzyme might occur due to enhanced activity of H_2O at the active site, again occurring concomitant with a tightening of the transition state structure relative to the acetyl-enzyme- H_2O complex. In order to specify the detailed mechanism for the Ca^{2+} more information concerning the structure and behavior of the enzyme is required. Specifically, knowledge of the primary, secondary, and higher order structure of the molecule would appear necessary. In addition, perhaps using X-ray crystallographic methods,

information concerning the changes in atomic and molecular articulations associated with the binding of substrates or other ligands would be of help in relating thermodynamic quantities describing overall effects to particular aspects of the protein. Recently, the use of transition-state substrate analogues for chymotrypsin and other enzymes has permitted correlation of activation energy parameter values with specific spatial alterations in active-site amino acids that participate in the reaction.

Until such detailed structural information becomes available, the possible mechanisms for Ca²⁺ acceleration reflected in thermodynamic and kinetic parameters must remain quite speculative.

C. Active site numbers and molecular forms of brain acetylcholinesterase

Accurate determination of the active-site numbers of different forms of acetylcholinesterase depends on the specificity of labelling of the reactive serine moieties at the active centers of the enzyme molecule and reliable removal of unreacted reagent. Rates of specific site phosphorylation should be orders of magnitude greater than those of non-specific site phosphorylation. Diisopropylfluorophosphate interacts with acetylcholinesterase more slowly than certain other phosphorylating agents, which is due in part to the absence of a quaternary nitrogen atom capable of association with the primary anionic component of the active site. Therefore to lessen non-specific site phosphorylation, the excessive exposure of acetylcholinesterase preparations to

³H di-isopropylfluorophosphate was avoided by terminating the reaction at the point of 98% inhibition of enzyme activity. The specificity of active-site labelling with ³H -diisopropylfluorophosphate was confirmed by its reversibility with pyridine-2-aldoxime which interacts with the primary anionic site to provide appropriate orientation of the oxime moiety relative to the phosphorylated serine residue of acetylcholinesterase (Wilson and Ginsburg, 1955). With such controls and by using Sephadex G-10 chromatography to remove excess of

³H -di-isopropylfluorophosphate, active-site numbers could be determined on acetylcholinesterase samples containing as little as 0.5 μ g of enzyme with reliability similar to that obtained with 1 μ g samples (10%).

Though acetylcholinesterase from mammalian brain has been investigated

less thoroughly than the enzyme from electric eel tissue, most studies have demonstrated a multiplicity of forms that differ in molecular weights (Jackson and Aprison, 1966; Chan et al., 1972; Hollunger and Niklasson, 1973; Adamson et al., 1975). It has been suggested that different forms of brain acetylcholinesterase may all be related to a single low-molecular weight form via aggregation processes (Adamson et al., 1975) and some evidence exists that such processes may be reversible (Viana, 1974) or preventable (Chan et al., 1976). In the present study, gel electrophoresis of bovine acetylcholinesterase preparations revealed the presence of an active form of the enzyme with an approximate molecular weight of 60000. This form is similar to the molecular weight of the smallest active form of pig brain acetylcholinesterase (McIntosh and Plummer, 1973) and slightly smaller than the low molecular weight species from mouse brain acetylcholinesterase (Adamson et al., 1975) and bovine brain acetylcholinesterase (Chan et al., 1976) when molecular weight estimates were made by G-200 chromatography.

The time course study of electrophoretic migration of form C (molecular weight 60000) suggests that a single molecular weight species, probably unchanged by the electrophoresis, is responsible for the observed enzyme stain. The observation of a 60000 molecular weight active species from eel electric tissue supports the suggestion that the 60000 molecular weight unit may be the basic unit in the eel acetylcholinesterase system as well.

Time course studies on electrophoretic migration of form B (240000 by G-200 chromatography) does not rule out dissociation

to form smaller species. Such an effect may provide an explanation for the observation that the 240000 molecular weight "form" behaves as forms of approximately 120000-140000 molecular weight when the molecular weights are estimated by gradient gel electrophoresis. Differences in hydrodynamic volume, or other physical factors might explain the differences in the molecular weight estimates. The observation that form B can be resolved into two enzyme staining bands of molecular weights estimated to be approximately 120000 and approximately 140000 respectively suggests the possibility of dissimilar subunits and possibly provides evidence for acetylcholinesterase isoenzymes. If the 120000 and 140000 molecular weight forms are not the result of dis-aggregation, a conclusion supported by the time course experiments, then the differences in molecular weights between the two forms could result from association of two identical smaller species in two different ways, resulting in different sieving behaviors, or two compositionally and/or structurally distinct smaller species associating to form the above two species. The latter possibility is suggestive of the existence of isoenzymes. However, choosing between the above possibilities or others must result from analysis of the composition and/or subunit behavior of the 120000 and 140000 molecular weight species.

D. Brain acetylcholinesterase multiple forms and Ca²⁺ acceleration

The multiplicity of brain acetylcholinesterase forms has been noted by others as referenced earlier. There have been suggestions that the larger molecular weight forms result from the association of low molecular weight forms and this effect has been specifically noted for the two forms examined thermodynamically and kinetically. Since the larger form appears to result from the smaller, the differences in kinetic behavior probably occurs as a result of molecular association of forms. The differences in kinetic behavior could provide a basis for co-operativity or interaction between the components of the larger species.

BIBLIOGRAPHY

1. Adamson, E. D., Ayers, S., Deussen, Z. A. and Graham, C. F. "Analysis of the Forms of Acetylcholinesterase from Adult Mouse Brain." Biochem. J., 147: 205-214, (1975).
2. Aldridge, W.N. "Some Properties of Specific Cholinesterase with Particular Reference to the Mechanism of Inhibition by Diethyl-p-Nitrophenylthiophosphate (E 605) and Analogues." Biochem. J., 46: 451-460, (1950)
3. Alles, G. A. and Hawes, R. C. "Cholinesterases in the Blood of Man." J. Biol. Chem., 133(2): 375-390, (1940)
4. Belleau, B., DiTullio, V. and Tsai, Y.-H. "Kinetic Effect of Leptocurares and Pachycurares on the Methanesulfonylation of Acetylcholinesterase." Mol. Pharmacol., 6: 41-45, (1970).
5. Bergmann, F., Wilson, I. B., and Nachmansohn, D. "Acetylcholinesterase: IX Structural Features Determining the Inhibition by Amino Acids and Related Compounds." J. Biol. Chem., 186: 693-703, (1950).
6. Bohlen, P., Stein, S., Dairman, W. and Udenfriend, S. "Fluorometric Assay of Protein in the Nanogram Range." Arch. Biochem. Biophys., 155: 213-220, (1973)
7. Breslow, E. and Gurd, F.R.N. "Reactivity of Sperm Whale Metmyoglobin towards Hydrogen Ions and p-Nitrophenyl Acetate." J. Biol. Chem., 237: 371-381 (1962).
8. Bruice, T. C. and Schmir, G. L. "The Influence of Mechanism on the Apparent pKa of Participating Groups in Enzymic Reactions." J. Am. Chem. Soc., 81: 4552-4556 (1959).
9. Butler, J. A. V. "The Molecular Kinetics of Trypsin Action." J. Am. Chem. Soc., 63: 2971-2974 (1941).
10. Caplow, M. "Chymotrypsin Catalysis: Evidence for a New Intermediate." J. Am. Chem. Soc., 91: 3639-3645 (1969).
11. Chan, S. L., Shirachi, D. Y., Bhargava, H. N., Gardner, E., and Trevor, A. J. "Purification and Properties of Multiple Forms of Brain Acetylcholinesterase." J. Neurochem., 19: 1747-2758.
12. Chan, S. L., Gordon, M. A., and Trevor, A. J. "Divalent Cations and the Molecular State of Brain Acetylcholinesterase." (in prep.) (1976).

13. Changeux, J. P. "Responses of Acetylcholinesterase from Torpedo marmorata to Salts and Curarizing Agents." Mol. Pharmacol., 2: 369-392 (1966).
14. Changeux, J. P., Podleski, T., and Meunier, J. C. "On Some Structural Analogies Between Acetylcholinesterase and the Macromolecular Receptor of Acetylcholine." J. gen. Physiol., 54: 225s-244s (1969).
15. Cornish-Bowden, A. "Estimation of the Dissociation Constants of Enzyme-Substrate Complexes from Steady-State Measurements." Biochem. J., 153: 455-461(1976).
16. Eccles, J. C. and MacFarlane, W.V. "Actions of Anti-cholinesterases on Endplate Potentials of Frog Muscle." J. Neurophysiol., 12: 59-80 (1949).
17. Eccles, J. C. and Jaeger, J. C. "The Relationship Between the Mode of Operation and the Dimensions of the Junctional Regions at Synapses and Motor End Organs." Proc. R. Soc. B., 148: 38-56 (1958).
18. Ellman, G.L., Bourtney, D., Andres, V. and Featherstone, R.M. "A New and Rapid Colorimetric Determination of Acetylcholinesterase Activity." Biochem. Pharmacol., 7: 88-95 (1961).
19. Fatt, P. and Katz, B. "Spontaneous Subthreshold Activity of Motor Nerve Endings." J. Physiol., 117: 109-128 (1952).
20. Fersht, A. R. and Requena, Y. "Mechanism of the Chymotrypsin-Catalyzed Hydrolysis of Amides:pH Dependence of k_c and K_m : Kinetic Detection of an Intermediate." J. Am. Chem. Soc., 93: 7079-7086 (1971).
21. Fersht, A. R. "Catalysis, Binding, and Enzyme-Substrate Complementarity." Proc. R. Soc. Lond. B., 187: 397-407 (1974).
22. Froede, H. C. and Wilson, I. B. "On the Subunit Structure of Acetylcholinesterase." Isr. J. Med. Sci., 6: 179-184 (1970).
23. Fromm, H. J. In: Initial Rate Enzyme Kinetics, Springer-Verlag, New York, pp 201-224 (1975).
24. Gardner, E. "Polyacrylamide Gel Electrophoresis and Proteins on a Micro-Scale." Proc. West. Pharmacol. Soc., 17: 135-137 (1974).
25. Gardner, E., Chan, S.L., Thorne, D. R., and Trevor, A.J. "Purified Mammalian Brain Acetylcholinesterase-A Glycoprotein." Biophys. J., 15: 50a (1975).

26. Glick, D. "Studies on the Specificity of Choline Esterase" J. Biol. Chem., 125: 729-739, (1938).
27. Gordon, M. A., Chan, S.-L., and Trevor, A. J. "Active Site Determinations on Forms of Mammalian Brain and Eel Acetylcholinesterase." Biochem. J., 157: 69-76 (1976).
28. Gutfreund, J. In: Enzymes-Physical Principles, Wiley Interscience, New York, pp 162-163 (1972).
29. Harris, L. W., Fleisher, J. H., and Clark, J. "Dealkylation and Loss of Capacity for Reactivation of Cholinesterase Inhibited by Sarin." Science, 154: 404-406 (1966).
30. Hartley, B. S and Kilby, B. A. "The Inhibition of Chymotrypsin by Di-ethyl p-Nitrophenyl Phosphate." Biochem. J., 50: 672-678 (1952).
31. Heilbronn, E. "Action of Fluoride on Cholinesterase I. On the Mechanism of Inhibition." Acta Chem. Scand., 19: 1333-1346 (1965).
32. Ho, I.K. and Ellman, G. L. "Triton Solubilized Acetylcholinesterase of Brain." J. Neurochem., 16: 1505-1513 (1969).
33. Hobbiger, F. "Effects of Nicotinhydroxamic Acid Methiodide on Human Plasma Cholinesterase Inhibited by Organo-Phosphates Containing a Dialkylphosphato Group." Br. J. Pharmacol., 10: 356-362 (1955).
34. Hollunger, E. G. and Niklasson, B. H. "The Release and Molecular State of Mammalian Brain Acetylcholinesterase." J. Neurochem., 20: 821-836 (1973).
35. Hoskin, F. C. G. and Trick, G. S. "Stereospecificity in the Enzymatic Hydrolysis of Tabun and Acetyl- β -Methylcholine Chloride." Can. J. Biochem & Physiol., 33: 963-969 (1955).
36. Jackson, R.L. and Aprison, M. H. "Mammalian Brain Acetylcholinesterase: Purification and Properties." J. Neurochem. 13: 1351-1365 (1966a) .
37. Jackson, R. L. and Aprison M.H. "Mammalian Brain Acetylcholinesterase: Effects of Surface Active Agents." J. Neurochem., 13: 1367-1371 (1966b).
38. Jencks, W. P. Catalysis in Chemistry and Enzymology, McGraw-Hill, New York (1969).
39. Jencks, W. P. and Page, M.I. "On the Importance of Togetherness in Enzymic Catalysis." In: Proc. Eighth FEBS Meeting, Amsterdam, 29: 45-58 (1972).

40. Jencks, W. P. "Binding Energy, Specificity and Enzymic Catalysis: The Circe Effect." In: Adv. in Enzymol., 43 (Interscience, New York, ed. A Meister) pp 219-410 (1975).
41. Kaplay, S. S. and Jagannathan, V. "Purification of Ox Brain Acetylcholinesterase." Indian J. Biochem., 3: 54-55 (1966).
42. Kaplay, S. S. and Jagannathan, V. "Purification and Properties of Ox Brain Acetylcholinesterase." Arch. Biochem. Biophys., 138: 48-57 (1970).
43. Katz, B. and Miledi, R. "Propagation of Electric Activity in Motor Nerve Terminals." Proc. R. Soc. B., 161: 453-482 (1965).
44. Katz, B. and Miledi, R. "Further Observations on Acetylcholine Noise." Nature New Biol., 232: 124-126 (1971).
45. Katz, B. and Miledi, R. "The Statistical Nature of the Acetylcholine Potential and its Molecular Components." J. Physiol., 224: 665-699 (1972).
46. Katz, B. and Miledi, R. "The Binding of Acetylcholine to Receptors and its Removal from the Synaptic Cleft." J. Physiol., 231: 549-574 (1973).
47. Kaufman, S., Neurath, H., and Schwert, G. W. "The Specific Peptidase and Esterase Activities of Chymotrypsin." J. Biol. Chem., 177: 793-814 (1949).
48. Kayne, F. J. and Suelter, C.H. "Effects of Temperature, Substrate, and Activating Cations on the Conformations of Pyruvate Kinase in Aqueous Solutions." J. Am. Chem. Soc., 87: 897-900 (1965).
49. Kitz, R. J., Braswell, L.M. and Ginsburg, S. "On the Question: Is Acetylcholinesterase an Allosteric Protein." Mol. Pharmacol., 6: 108-121 (1970).
50. Kremzner, L.T., Kitz, R. T., and Ginsburg, S. "A Partial Purification and Characterization of the Acetylcholinesterase of Human Blood." Fedn. Proc. Fedn. Am. Socs. Exp. Biol., 26: 296 (1967).
51. Lawler, H. C. "A Simplified Procedure for the Partial Purification of Acetylcholinesterase from Electric Eel." J. Biol. Chem., 234: 799-801 (1959).
52. Leuzinger, W. "The Number of Catalytic Sites in Acetylcholinesterase" Biochem. J., 123: 139-141 (1971).
53. Marini, J.L. and Caplow, M. "Substrate Induced pK Perturbations with Chymotrypsin." J. Am. Chem. Soc., 93: 5560-5566 (1971).

54. Marnay, A. and Nachmansohn, D. "Cholinesterase in Voluntary Frog's Muscle." J. Physiol., 89: 359-367 (1937).
55. Marquis, J. K. and Webb, G. D. "Interactions of Calcium with Purified and Intact Cell Acetylcholinesterase of Electrophorus electricus." Biochem. Pharmacol., 23: 3459-3465 (1974)
56. McIntosh, C.H.S. and Plummer, D. T. "Multiple Forms of Acetylcholinesterase from Pig Brain." Biochem. J., 133: 655-665 (1966).
57. Mitchell, P. "Reversible Coupling Between Transport and Chemical Reactions" In: Membrane and Ion Transport vol. 1 (ed. E. Bittar, Wiley-Interscience, New York) pp 194-195 (1971).
58. Monod, J. Wyman, J. and Changeux J. P. "On the Nature of Allosteric Transition: A Plausible Model." J. Mol. Biol., 12: 88-118 (1965).
59. Murdoci, A. L., Grist, K. L., and Hirs. C.H.W. " On the Dinitrophenylation of Bovine Pancreatic Ribonuclease A-Kinetics of the Reactions in Water and Urea." Arch. Biochem. Biophys., 114: 375-390 (1966).
60. Nachmansohn, D. and Rothenberg, M. "On the Specificity of Choline Esterase in Nervous Tissue." Science, 100: 454-455 (1944).
61. Ord, M.G. and Thompson, R.H.S. "The Preparation of Soluble Cholinesterases from Mammalian Heart and Brain." Biochem. J., 49: 191-199 (1951).
62. Ottolenghi, P "The Effects of Hydrogen Ion Concentration on the Simplest Steady-State Enzyme Systems." Biochem. J., 123: 445-453 (1971).
63. Page, M. I. and Jencks. W. P. "Entropic Contributions to Rate Accelerations in Enzymic and Intramolecular Reactions and the Chelate Effect." Proc. Natl. Acad. Sci. USA., 68: 1678-1683 (1971).
64. Porter, C. W. and Barnard. E. A. "The Density of Cholinergic Receptors at the Endplate Post-Synaptic Membrane: Ultrastructural Studies in Two Mammalian Species." J. Membrane Biol., 20: 31-49 (1975)
65. Renard, M. and Fersht, A. R. "Anomalous pH Dependence of k_{cat}/K_m in Enzyme Reactions: Rate Constants for the Association Chymotrypsin with Substrates." Biochemistry, 12: 4713-4718 (1973)

66. Rosenberry, T. R. "Catalysis by Acetylcholinesterase: Evidence that the Rate Limiting Step for Acylation with Certain Substrates Precedes General Acid-Base Catalysis." Proc. Natl. Acad. Sci. USA. ,72:3834-3838 (1975).
67. Roufogalis, B. D. and Thomas, J "The Acceleration of Acetylcholinesterase Activity at Low Ionic Strength by Organic and Inorganic Cations." Mol. Pharmacol. ,4:181-186 (1968).
68. Roufogalis, B. D. and Quist, E.E. "Relative Binding Sites of Pharmacologically Active Ligands on Bovine Erythrocyte Acetylcholinesterase." Mol. Pharmacol. ,8:41-49 (1972).
69. Roufogalis, B. D. and Wickson, V. M. "Specific Inactivation of Allosteric Effects by a Water-Soluble Carbodiimide." J. Biol. Chem. ,248:2254-2256 (1973).
70. Schaffer, N.K., Norwood, K.S., May, S.C. and Summerson, W.H. "Serine phosphoric acid from DFP-Chymotrypsin." J. Biol. Chem. ,202:67-76 (1953).
71. Schimerlik, M.I. and Cleland W. W. "Inhibition of Creatine Kinase by Chromium Nucleotides." J. Biol. Chem. ,248:8418-8423 (1973).
72. Schmidt, D. E. and Westheimer, F. H. "pK of the Lysine Amino Group at the Active Site of Acetoacetate Decarboxylase" Biochemistry , 10:1249-1253 (1971).
73. Schirachi, D. Y., Chan, S.-L., and Trevor, A. J. "Zonal Ultracentrifugation of Lubrol Extracted Na-K ATPase and AChEsterase from Bovine Brain." Pharmacologist ,12:521 (1970).
74. Segel, I.H. In: Enzyme Kinetics-Behavior and Analysis of Rapid Equilibrium and Steady-State Enzyme Systems (Wiley Interscience, New York) pp. 938-940 (1975)
75. Snoke, J. E. and Neurath, H. "The Effect of Temperature on the Esterase Activity of Chymotrypsin." J. Biol. Chem. ,182:577-584 (1950).
76. Spencer, T. and Sturtevant, J. M. "The Mechanism of Chymotrypsin Catalyzed Reactions." J. Am. Chem. Soc. , 81:1874-1882 (1959).
77. Tanford, C. In: Physical Chemistry of Macromolecules (Wiley-Interscience, New York) pp. 574-577 (1961).
78. Taylor, P. and Lappi, S. "Interaction of Fluorescence Probes with Acetylcholinesterase-Site and Specificity of Propidium Binding." 14: 1989-1997 (1975).

79. Uriel, J. "Characterization of Enzymes in Specific Immune-Precipitates." Ann. N. Y. Acad. Sci., 103: 956-979 (1963).
80. Vahlquist, B. "On the Esterase Activity of Human Blood Plasma." Scand. Arch. Physiol., 72: 133-160 (1935).
81. Wilson, I. B. "Acetylcholinesterase: Further Study of Binding Forces." J. Biol. Chem., 197: 215-225 (1952).
82. Wilson, I. B. and Bergman, F. "Studies on Cholinesterase: VII The Active Surface of Acetylcholine Esterase Derived from Effects of pH on Inhibitors." J. Biol. Chem., 185: 479-489 (1950a).
83. Wilson, I. B. and Bergman, F. "Acetylcholinesterase: VIII Dissociation Constants of the Active Groups." J. Biol. Chem., 186: 683-692 (1950b).
84. Wilson, I. B., Bergman, F. and Nachmansohn, D. "Acetylcholinesterase: Mechanism of the Catalysis of Acylation Reactions." J. Biol. Chem., 186: 781-790(1950).
85. Wilson, I. B. and Cabib, E. "Acetylcholinesterase: Enthalpies and Entropies of Activation." J. Am. Chem. Soc., 78: 202-207, (1956).

APPENDICIES

Statistical Tests

Paired observation test

This test was used to compare values of activation energy parameters in the presence and absence of Ca^{2+} at different pH values. The purpose was to determine if changes, in the presence of Ca^{2+} , in values of activation parameters were statistically significant.

The "t" value was calculated from the following relationship:

$$t = \frac{\bar{d}}{\text{S. E.}}$$

\bar{d} is the mean difference between the pairs of values of, e.g., ΔG^\ddagger obtained with and without Ca^{2+} . If x were the value of ΔH^\ddagger in the absence of Ca^{2+} and x' the value in the presence of Ca^{2+} , then $(x-x') = d$. N is the number of data pairs. The standard error, S. E., was calculated from the following relationship:

$$\text{S. E.} = \sqrt{\frac{(\sum (d-\bar{d})^2)}{N(N-1)}}$$

Confidence interval of the slope of an asymptote drawn from points on a line which were extrapolated from experimental points

As indicated in the text, the asymptote drawn to the curved Arrhenius plot, on occasion required extrapolation beyond the data points. The procedure utilized to determine the "y" values (log k) for extrapolated "x" values (1/T) was as follows:

The standard deviation (S.D.) of the best fit line drawn through the data points was first calculated.

$$\text{S.D.} = \sqrt{\frac{\sum (Y_{\text{exp}} - Y_{\text{fit}})^2}{N(N-2)}}$$

where Y_{exp} is the value of an experimental point and Y_{fit} is the value on the line fitted to the set of data points.

The confidence interval determined from standard error (S.E.) of "y" at an extrapolated point "x" is given by:

$$\text{S.E.} = \sqrt{(\text{S.D.})^2 \left\{ \frac{1}{N} + \frac{(x_{\text{ext}} - \bar{x})^2}{\sum (x_{\text{exp}} - \bar{x})^2} \right\}}$$

where x_{ext} is the value of x at a point extrapolated from the data point region of the curve and \bar{x} is the average value of the experimental x values. If the above process is done for two extrapolated "y" values and their corresponding "x" values then $y_1 \pm \text{S.E. for } x_1$

and $y \pm S. E.$ for x can be determined. From these two points and their standard errors, lines may be drawn with the confidence limit established. From the two lines, both representing $\log k$ vs. $(1/T)$ values of rate constants at a given temperature can be calculated and the accuracy of the estimate determined. The X-axis extrapolation was no more than about $5^\circ C$ beyond the measured values.

For determination of the correlation coefficient used throughout the study, the following relationship was employed.

$$C.C. = \frac{\sum (y - \bar{y})^2 - \sum (y - y_{\text{fit}})^2}{\sum (y - \bar{y})^2}$$

where y is an experimental point, \bar{y} is the average of the experimental y points and y_{fit} is the value of y on the curve or line fit to the data points

Richard D. Remington and M. Anthony Schork,
Statistics with Applications to the Biological and Health Sciences

Prentice Hall, N. J. (1970)

Determination of pK values

pK values may be estimated from plots of $\log V_{\text{max. app.}}$ versus pH according to Dixon (1964). This method is based on a system which has two pK values over approximately 3 pH units apart. The relationship between the $\log V_{\text{max. app.}}$ (experimental)

and the theoretical V_{max} is given by:

$$\log V_{\text{max. app.}} = \log V_{\text{max.}} - \log \left[\left(1 + \frac{(H^+)}{K_{\text{es1}}} + \frac{K_{\text{es2}}}{(H^+)} \right) \right] \quad (1)$$

where K_{es1} is the ionization constant of the enzyme at low pH (e.g. 5-8) and K_{es2} refers to the ionization state at the higher pH values. At the low pH values, the $K_{\text{es2}} / (H^+)$ may be ignored, since it refers to an ionization state not significantly present at the low pH. Since $(H^+) / K_{\text{es1}}$ is usually greater than 1 in the above equation, the 1 can be ignored. The resulting expression is:

$$\log V_{\text{max. app.}} = \log V_{\text{max.}} - \log \frac{(H^+)}{K_{\text{es1}}} = \quad (2)$$

$$\log V_{\text{max.}} + \text{pH} - \text{p}K_{\text{es1}} \quad (3)$$

At low pH values, the plot starts off as a straight line with a slope of +1. At a point on this line where $V_{\text{max. app.}} = V_{\text{max}}$,

$\log (V_{\text{max. app.}} / V_{\text{max}}) = 0$ and thus $\text{pH} = \text{pK}_{\text{esl}}$. To

obtain pK_{esl} , a horizontal line at V_{max} and a line of slope = 1,

tangent to the plot at low pH may be drawn. The horizontal coordinate of the intersection points give the pK_{esl} when this intersection

point is 0.3 pH units above the reference point on the pH curve.

Ideal ionization curves

The relationship for enzymatic rates and pH is given by Dixon (1964) as follows:

$$\text{pH} - \text{pK} = \log \left(\frac{1}{\frac{k_{\text{max}}}{k} - 1} \right) \quad (4)$$

Since by previously discussed methods, the pK has been determined

(see above) and the value of k_{max} ($=V_{\text{max}}/E$) determined, the

theoretical value of k may be calculated for any pH with the above equation (4). A plot through these points represents the ideal ionization curve and can be compared with the curve drawn through the experimental points.

Hyperbolic fitting program for Km determinations

On the following two pages is the hyperbolic fitting program used in this study for estimation of K_m values. It has been slightly modified from the original published form given by Cleland (1967) for use with the IBM 370/145 series computer employed since January, 1976 at the University of California Medical Center, San Francisco.

In the current program format for use with either ATS or cards, the first ATS line or card indicates the number of data pairs (e. g. if there are 7 velocity-substrate values, the card would read 007; for 150 such pairs, 150). Following this entry, each subsequent ATS line or card gives velocity and substrate information of the form:

V. VVVVVVVV, S. SSSSSSSS, where the V and S values correspond to the velocity and substrate values. Note that there are 10 total spaces assigned to each of the V and S designations with 1 space to the left of the decimal point and 8 to the right of the decimal point. At the conclusion of the data set a blank ATS line or card indicates the termination of data input. The sequence of information for the computer run is as follows:

1. JCL (job command language) -conforming to format designated in the IBM manuel)
2. the cleland program
3. \$entry line or card
4. data
5. \$stop
6. Run command (rje from ATS, i. e. remote job entry)

Cleland, W. W. "The Statistical Analysis of Enzyme Kinetic Data." From Advances in Enzymology, 29 (ed. F. F. Nord, Wiley, Interscience: New York) pp. 1-32 (1967).

DIMENSION V(100), A(100), W(100), S(3,4), O(3), SM(3), SS(3)
Print 100

```

100 FORMAT (36H FIT TO HYPERBOIA      V=VMAX*A/(K+A))
11  FORMAT(13,17X,31H RESULTS PRINTED HERE ON OUTPUT)
1   FORMAT (F10.8,1X,F10.8,1X,F10.8)
    JJ=0
14  READ 11, NP
    IF (NP) 99, 99, 12
12  M=1
    N=2
    P=NP-M
    N1=M+1
    N2=N+2
    GO TO 2
16  CK=S(1,1)/S(2,1)
    JJ=JJ+1
    PRINT 11, JJ
    NT=0
    M=2
    GO TO 2
18  CK=CK-S(2,1)/S(1,1)
    NT=NT+1
    IF (NT-3) 2, 21, 21
21  S2=0
    DO 22 I=1, NP
22  S2=S2+(V(I)-S(1,1)*A(I)/(CK+A(I)))**2*W(I)
    S2=s2/P
    S1=SQRT(S2)
    SI=CK/S(1,1)
    VINT=1.0/S(1,1)
    VK=1.0/SI
    DO 10 J=2, N1
    DO 10 K=1, N
10  S(K, J)=S(K, J)*SM(K)*SH(J-1)
    SEV=S1*SQRT(S(1,2))
    SECK=S1*SQRT(S(2,3))/S(1,1)
    SEVI=SEV/S(1,1)**2
    S(1,3)=S1*SQRT(CK**2*S(1,2)+S(2,3)+2.0*CK*S(1,3))
    SEFL=S(1,3)/S(1,1)**2
    SEVK=S(1,3)/CK**2
    WCK=1.0/SECK**2
    WV=1.0/SEV**2
    WSL=1.0/SEFL**2
    WVI=1.0/SEVI**2
    WMK=1.0/SEVK**2
    PRINT 30, CK, SECK, WCK
    PRINT 31, S(1,1), SEV, WV
    Print 32, SI, SEFL, WSL
    Print 33, VINT, SEVI, WVI
    PRINT 34, VK, SEVK, WMK
    Print 35, S2, S1
30  FORMAT (7H K      = , F12.6, 13H S.E.(K)   = , F11.6, 5H W = , F14.5)
31  FORMAT(7H V      = , F12.6, 13H S.E.(V)   = , F11.6, 5H W = , F14.5)
32  FORMAT(7H K/V    = , F12.6, 13H S.E.(K/V) = , F11.6, 5H W = , F14.5)
33  FORMAT(7H 1/V    = , F12.6, 13H S.e.(1/V) = , F11.6, 5H W = , F14.5)
34  FORMAT(7H V/K    = , F12.6, 13H S.E.(V/K) = , F11.6, 5H W = , F14.5)
35  FORMAT(12H VARIANCE = , F14.5, 10H SIGMA = , F12.7)
    GO TO 14
2   DO 3 J=1, N2
    DO 3 K=1, N1
3   S(K, J)=0
    DO 4 I=1, NP

```

```


15 READ 1, V(1), A(1), W(1)
   IF (V(1)) 19, 19, 20
19 W(1)=1
20 O(1)=V(1)**2/A(1)
   O(2)=V(1)**2
   O(3)=V(1)
   GO TO 13
17 D=CK+A(1)
   O(1)=A(1)/D
   O(2)=O(1)/D
   O(3)=V(1)
   GO TO 13
13 DO 4 J=1, N1
   DO 4 K=1, N
4   S(K, J)=S(K, J)+O(K)*O(J)*W(1)
   DO 5 K=1, N
5   SM(K)=1.0/SORT(S(K, K))
   SM(N1)=1.0
   DO 6 J=1, N1
   DO 6 K=1, N
6   S(K, J)=S(K, J)*SM(K)*SM(J)
   SS(N1)=-1
   S(1, N2)=1
   DO 8 L=1, N
   DO 7 K=1, N
7   SS(K)=S(K, 1)
   DO 8 J=1, N1
   DO 8 K=1, N
8   S(K, J)=S(K+1, J+1)-SS(K+1)*S(1, J+1)/SS(1)
   DO 9 K=1, N
9   S(K, 1)=S(K, 1)*SM(K)
   GO TO (16, 18), N
36 FORMAT(23H PROGRAM COMPLETED FOR , I4, 6H LINES)
99 PRINT 36, JJ
   STOP
   END

```




FOR REFERENCE

NOT TO BE TAKEN FROM THE ROOM

 CAT. NO. 23 012

PRINTED
IN
U.S.A.

